Chapter 3

Role of carbon concentration and mode of cultivation on growth and accumulation of lipid, starch, and photosynthetic pigments in *Chlamydomonas reinhardtii* under heterotrophy and mixotrophy

Salient features of bioenergy production under hetero/mixotrophy in *C. reinhardtii*

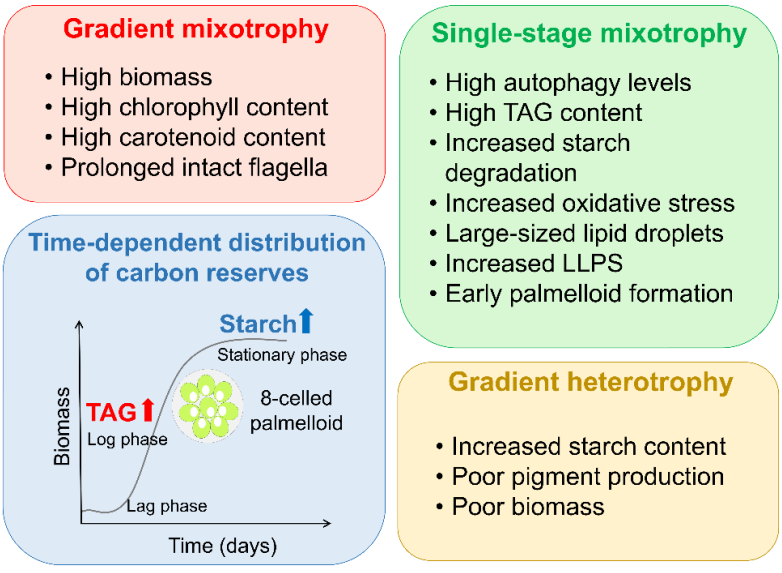

3 Role of carbon concentration and mode of cultivation on growth and accumulation of lipid, starch, and photosynthetic pigments in *Chlamydomonas reinhardtii* under heterotrophy and mixotrophy

3.1 Abstract

Heterotrophic and mixotrophic growth of microalgae can also lead to increased cell density and biofuel production. In this study, a novel strategy of gradient addition of carbon source is used in C*hlamydomonas reinhardtii* CC-125 to obtain better cell count yields. Sodium acetate at 5 g/L was found to be the best condition for good cell density and lipid production. Gradient strategy substantially enhanced cell density. Gradient mixotrophy yielded the highest cell density of 0.74 ± 0.004 million cells/mL after 10 days of cultivation and exhibits low levels of autophagy. This approach also enhances the chlorophyll (36.17 ± 1.74 mg/mL) and carotenoids (8.85 ± 0.52 mg/mL) production in mixotrophy. At 5 g/L sodium acetate, the gradient mode resulted in increased starch accumulation at the stationary phase, while the single-stage produces the maximum triacylglycerol (TAG) content at the log phase in both the trophic modes. While heterotrophy yielded the highest content of starch, mixotrophy resulted in high TAG production. TAG production is correlated with autophagy, de-novo lipid synthesis, and starch degradation process. Increased autophagy seems to indicate high oxidative stress in the single stage which results in liquid-liquid phase separation (LLPS) of TAG from the cytosol, forming lipid droplets (LDs) for cellular redox maintenance. The LD-cytosol phase coexistence boundary for single-stage revealed complete LD demixing from cytosol above a saturated area fraction (φ_{sat}) due to LD growth. In the gradient mode, LDs are small and dispersed in the cytosol. These differences in LD size and density are attributed to the cell's proteome and thermodynamic factors. For the first time, LLPS is observed to influence LD biogenesis in *C. reinhardtii*. Overall, this study unravels the metabolic regulation of mixotrophic biofuel production in *Chlamydomonas* and demonstrates the gradient strategy of hetero/mixotrophic cultivation as a promising approach for improving the yields of various bioenergy products.

3.2 Introduction

Green microalgae are capable to grow non-photosynthetically in the presence of an organic carbon source like acetate (Harris, 2001). Studies have shown that among the three modes of cultivating microalgae, heterotrophy and mixotrophy enhance biomass production more than the autotrophic mode (S. Kim et al., 2013) which is useful for wastewater and agricultural waste treatment (da Silva et al., 2021; Msanne et al., 2020).

Several studies have revealed that heterotrophy results in rapid utilization of nutrients present in the medium and hence a faster growth rate in comparison to mixotrophy (Jin et al., 2020; Perez-Garcia et al., 2011). A study on *Chlamydomonas reinhardtii* suggests that acetate assimilation is faster in heterotrophy than in mixotrophy (Singh et al., 2014). The active metabolism of heterotrophs in the absence of light also minimizes the number of concerns while building a fermenter (Lowrey et al., 2015). Heterotrophic cultivation also results in enhanced lipid accumulation. In *Chlorella protothecoids*, heterotrophic cultivation using 10 g/L glucose resulted in 55% lipid accumulation as compared to only 15% under autotrophy (Miao & Wu, 2006). *Scenedesmus obliquus* produced maximum lipid content with 10 g/L glucose in heterotrophic mode (Nicodemou et al., 2022). However, due to the lack of light reaction of photosynthesis, this mode limits the production of chlorophyll and carotenoids, and hence the high-value phytochemicals (Lowrey et al., 2015). Loss of up to 94% chlorophyll has been observed in heterotrophic *C. protothecoids* (Xiong et al., 2010). Wang *et al.* demonstrate that the production of astaxanthin depends on carbon metabolism efficiency. While supplementing glucose increases the growth rate and hence astaxanthin accumulation, lactose, acetate, fructose, or sucrose decreases the production (Y. Wang & Peng, 2008).

However, few reports claim otherwise, for example, the mixotrophy mode in *Chlorella minutissima* and *Chlamydomonas globosa* causes a 2-7 times increase in biomass than either the heterotrophy or autotrophy modes (Bhatnagar et al., 2011). *Chlorella sorokiniana* yields as high as 51% lipid content during mixotrophy with glucose (Wan et al., 2011). Acetate mixotrophy increases the production of astaxanthin in *Haematococcus pluvialis* twice compared to heterotrophy (Cai et al., 2008). Proper selection of the carbon source is also important. For example, sucrose in *Chlorella* sp. Y8-1 and acetate in *Chlamydomonas* sp. increase biomass and lipid production (Lin &

Wu, 2015; Moon et al., 2013). Mixotrophic growth of *Chlorella* sp. with orange peel produces increased biomass and fatty acid methyl esters (FAMEs) (Park et al., 2014).

Majorly, the method of cultivation used to grow microalgae involves a single-stage approach, where the media supplements start to deplete towards the stationary phase and limit bioenergy feedstock production (R. Puzanskiy et al., 2021; Singh et al., 2014). In the past few years, two-stage cultivation has emerged as a promising method for high-value product formation (Aziz et al., 2020; Liyanaarachchi et al., 2021). Two-stage mixotrophy in *Chlorella vulgaris* enhances the biomass by 1.6-fold in the presence of glucose (Yen & Chang, 2013) and lutein (carotenoid) production in the presence of sodium acetate (C. Y. Chen & Liu, 2018; J. H. Chen et al., 2021). The two-stage heterotrophic autotrophic method improves the growth rate, cell density, and lipid productivity in *Chlorella sorokiniana* (Zheng et al., 2012). Stepwise increment of carbon source is the latest cultivation strategy adopted to further enhance production. The stepwise addition of glucose to the heterotrophic culture of *Scenedesmus acuminatus* enhances biomass production (Jin et al., 2020). Constant feeding of sodium acetate to the mixotrophic culture of *C. sorokiniana* showed increased lutein accumulation (Ma et al., 2020). So far, only a few studies have focused on these modes of heterotrophic/mixotrophic cultivation and hence require deeper attention.

The overall increased growth rate observed in heterotrophy/mixotrophy cultures is due to increased respiration and low photosynthetic rate (Chapman et al., 2015). In the case of mixotrophy, upon exhaustion of the carbon supply, the culture enters the autotrophy mode, thereby activating the photosynthetic machinery and hence starch production (J. H. Chen et al., 2021; Ran et al., 2019). In addition, if the carbon source is acetate, it is subjected to acetyl-CoA production followed by fatty-acid synthesis with the help of the acetyl-CoA carboxylase enzyme (ACC) (Goncalves et al., 2016). Increased fatty-acid production enhances the formation of neutral lipid molecules, i.e., triacylglycerol (TAG) with the help of diacylglycerol acyltransferase (DGAT) (Li-Beisson et al., 2015). Apart from the de-novo synthesis, catabolic pathways like autophagy and carbon partitioning also participate in TAG production (Fan et al., 2012; Li-Beisson et al., 2021). However, it is unclear how these enzymes and pathways respond to different metabolic signals generated by changing the mode of cultivation when microalgae are grown under hetero/mixotrophy.

TAG molecules produced by microalgal cells are known to accumulate in the core of membrane-less vesicles called lipid droplets (LD). LDs in *Chlamydomonas* are primarily cytosolic, however, they undergo compartmentalization as a result of a stressful environment (Henne et al., 2020; Li-Beisson et al., 2021). While the initial formation of LD is regulated by an ER protein called seipin, the growth of LDs is regulated by the combined actions of ARF1 and COP-I protein machinery present on the ER membrane (Walther et al., 2017). Bigger LDs in the cytosol grow at the expense of smaller droplets due to Ostwald ripening. Nucleation can also lead to droplet growth (Hyman et al., 2014). Stressful conditions, too, dictate the size and the density of lipid droplets (H. S. Kim et al., 2016; Walther et al., 2017). Several questions concerning the conditions which influence the LD formation dynamics, or the mechanism of LD growth dynamics remain unanswered.

In this chapter, wanted to understand the effect of the concentration of the externally added sodium acetate on the growth dynamics and bio-product formation in *Chlamydomonas reinhardtii* CC-125 is presented. The gradient strategy of adding sodium acetate in mixotrophy mode is developed and the impact on microalgal metabolism is analyzed. The anabolic, as well as catabolic pathways responsible for lipid production, were analyzed under such conditions. Our findings signify the increased growth rate in mixotrophy compared to heterotrophy or autotrophy modes. Finally, with the help of single-cell fluorescence microscopy, liquid-liquid phase separation in lipid droplet biogenesis was studied. How the autophagic mechanism alters the total cell count, starch, and lipid production in the gradient mode of cultivation, was addressed. The dependence of droplet dynamics on the mode of cultivation and stress application was assessed. Thus, this study focused on important features of microalgal metabolism under single-stage and gradient modes of mixotrophy cultivation which can help the development of large-scale production of bioenergy feedstock.

3.3 Materials and Methods

3.3.1 Microalgal growth conditions

Chlamydomonas reinhardtii CC-125 was procured from Chlamydomonas Resource Centre, Minnesota, USA. Microalgal cells were grown and maintained on Tris-acetate-

phosphate (TAP) medium pH 7.0, as described in the Section 2.3.1. In this study, we used sodium acetate (NaAc) as a carbon source for the heterotrophic (H) and mixotrophic cultivation (M) of *C. reinhardtii*.

3.3.2 Heterotrophic and mixotrophic cultivation strategies of *C. reinhardtii*

Heterotrophic cultivation was carried out in the absence of light and the presence of NaAc. In single-stage (SS) mode, NaAc was added only once at the beginning of cultivation on day 0, at a final concentration of 1 g/L, 5 g/L, and 10 g/L, named SS_H 1 gL^{-1}, SS_H 5 gL^{-1}, and SS_H 10 gL^{-1}, respectively. In the gradient mode (G) of cultivation, NaAc was added in small steps of fixed concentration at a definite time interval. Three different step sizes were chosen to understand their effect on growth and biofuel production, *viz*. 1) 0.5 g/L NaAc was added on each day of growth until the final concentration of 5 g/L was achieved (G_H 0.5_10); lowest step size of, 2) 1 g/L NaAc was added on alternate days of growth until the final concentration of 5 g/L was achieved (G_H 1_10), and 3) 1 g/L NaAc was added on each day of growth until the final concentration of 5 g/L was achieved (G_H 1_5) (**Figure 3.1**).

In the case of mixotrophic cultivation, the single-stage addition of NaAc was performed similarly to the heterotrophic mode. In the gradient mode (G) of cultivation, NaAc was added in small steps of fixed concentration at a definite time interval. Here, 1 g/L NaAc was added every 2nd day of cultivation to attain the final concentration of 5 g/L, namely G_M 5 gL^{-1} (**Figure 3.1**). Here, G_M 5 gL^{-1} is the same as the G_H 1_10 of the heterotrophic cultivation.

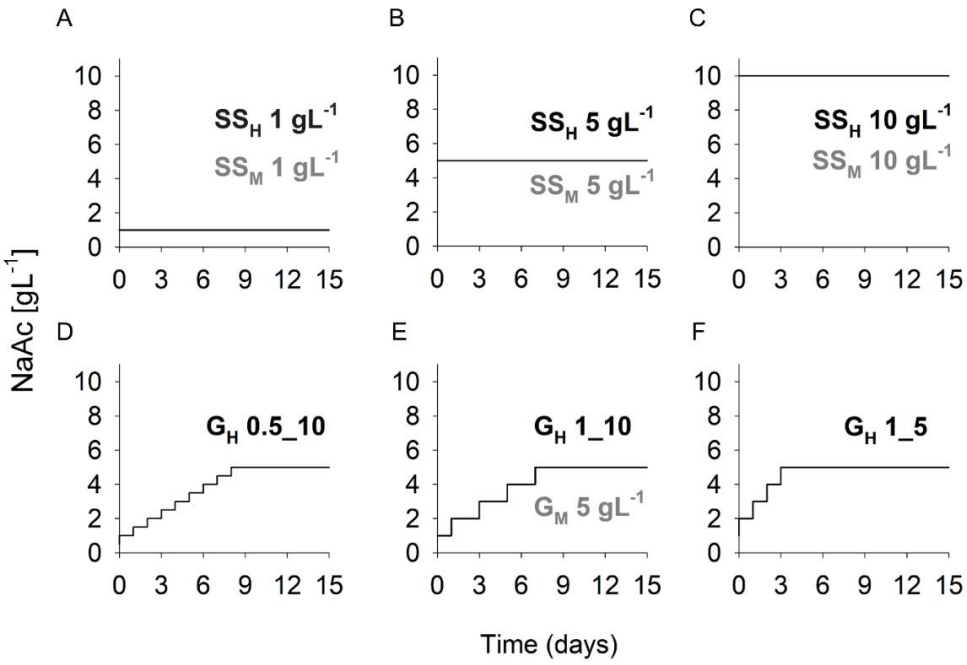

Figure 3.1. A schematic representation of hetero/mixotrophy cultivation strategies employed on *C. reinhardtii*.

A-C. Single-stage addition of sodium acetate at a concentration of 1 g/L, 5 g/L, and 10 g/L, respectively, was achieved at the commencement of cultivation. **D-F.** Gradient mode of cultivation showing fixed steps where 0.5 g/L NaAc was added every day (D), 1 g/L NaAc was added every 2nd day of growth (E), and 1 g/L NaAc was added every day (F) until the final concentration of 5 g/L was achieved. Here, "SS" stands for single-stage, "G" for gradient, "H" in the subscript means heterotrophy, and "M" means mixotrophy.

3.3.3 Measurement of cell density and growth parameters in *C. reinhardtii*

The microalgal cell density was performed using the universal equation (**Equation 3.1**) derived using a haematocytometer, as described in the Sections 2.3.3 & 2.4.1.

$$Cells\left(\times\frac{10^6}{mL}\right)=\frac{OD_{680}-0.015}{3.64}$$

Equation 3.1. Linear correlation of OD_{680} and cell density in million cells/mL.

The specific growth rate (μ) was acquired by fitting the growth curves using a sigmoidal function in OriginPro 9.0 software. The growth lag time was obtained by extrapolating the linear fit of the exponential phase of the growth curve on the x-axis (as shown for the Control, **Figure 3.2**). This x-intercept gives the value of lag time. Also, the doubling time of microalgal cells was calculated from μ using **Equation 3.2**.

$$Doubling\ time\ (DT)=\ {}^{ln2}/_{\mu}$$

Equation 3.2. The equation to calculate doubling time of *C. reinhardtii*

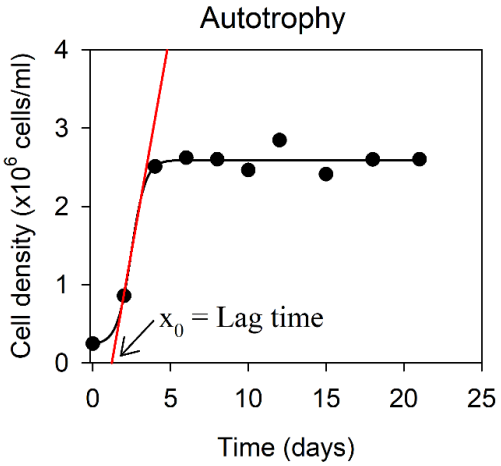

Figure 3.2. Growth curve fitting of the autotrophic control to determine lag time.

The black solid line passing through the scatter plot represents the growth/sigmoidal fit. The red line represents the linear fit of only the exponential phase of growth. This linear fit gives the value of the specific growth rate, which is equal to the slope of the line. X-intercept, x_0, gives the lag time of the culture.

3.3.4 Analysis of total photosynthetic pigments

C. reinhardtii cells were harvested at definite time points and resuspended in 95% ethanol. The carotenoids and chlorophyll (green-colored photosynthetic pigments) were extracted in the organic solvent, and the bleached-out cells were separated by centrifugation at 12,000 x g for 5 min (Cakmak et al., 2012). The solubilized pigments were estimated by measuring the absorbance at 470 nm (OD_{470}), 648 nm (OD_{648}), and 664 nm (OD_{664}), using a UV-Visible spectrophotometer (UV-1800, Shimadzu). The total chlorophyll and total carotenoid content in mg/mL and mg/10^6 cells were calculated using **Equations 2.1 to 2.6** (as mentioned in the Section 2.3.4 (Khan & Mitchell, 1987).

3.3.5 Estimation of total starch content using Lugol's iodine

The total starch content produced by the microalgal cells was estimated using Lugol's iodine (Black et al., 2013). Briefly, cells were first bleached by washing with 95% ethanol and then incubated at 100 ℃ along with Lugol's solution for 15 min to solubilize the cellular starch. After cell lysis, the cell debris was removed by centrifugation at 10,000 x g for 2 min. The solubilized starch was estimated in the form of starch-Lugol's complex at 595 nm (OD_{595}) in a multi-mode microplate reader (BioTek Synergy HT, now called Agilent) with path-length correction of 1 cm. The final starch content was obtained in arbitrary units (a.u.) per mL (a.u. /mL) and a.u. per 10^6 cells, after normalizing the absorbance with the experimental controls.

3.3.6 Triacylglycerol estimation using Nile red fluorescence

Triacylglycerol molecules present in the form of lipid droplets inside the cells were stained by Nile red dye. The cells were incubated for 10 min at 25 ℃ in dark with Nile red dye solution in DMSO at a final concentration of 1 µg/mL (W. Chen et al., 2009; Kou et al., 2013). The fluorescence of the Nile red-TAG complex was captured using a filter set with λ_{ex} = 485 ± 20 and λ_{em} = 590 ± 35 in a multi-mode microplate reader (BioTek Synergy HT, now called Agilent). The final TAG concentration was calculated in fluorescence units (f.u.) per mL and f.u. per 10^6 cells after normalizing the readings with the experimental controls.

3.3.7 Live-cell fluorescence imaging of lipid droplets

Lipid droplets were stained with 1 µg/mL Nile red dye, as described in the previous section. Post-staining, cells were observed with Olympus BX53F2 upright optical microscope in epifluorescence mode, using a 130 W U-HGLGPS excitation source, TRITC filter, and 100X (1.4 NA) Olympus oil-immersion objective. In all the measurements, ~100 cells were imaged with an Olympus DP74 camera for SS_M 5 gL^{-1} and G_M 5 gL^{-1}. An autotrophic control was also recorded for reference.

All the images were processed using Image J software (Fiji). Briefly, individual cells were selected and analyzed for the total fluorescence intensity of a cell (pixels), size of the lipid droplets (μm^2) contained in a cell, size of the cell (μm^2), and fluorescence intensity of the lipid droplets occupying the cell (pixels), using a custom-made program. The percent area of the cell occupied by lipid droplets (φ) was calculated for LLPS analysis.

3.3.8 Total RNA extraction and quantitative real-time PCR

The RNA extraction was done using the TRI Reagent from Sigma-Aldrich Pt. Ltd. as described by Bell et al. (2016). Here, ~5×10^6 *Chlamydomonas* cells were homogeneously mixed in TRI Reagent and the mixture was subsequently treated with chloroform. The total RNA extracted in the aqueous layer was then precipitated by isopropanol; the precipitated RNA pellet was washed with chilled 70% ethanol and treated with DNase I (final concentration, 1 U) at 37 ℃ for 40 min. The total RNA was quantified using a Nano-spectrophotometer. A total of ~1 µg of RNA was converted to cDNA using Anchored Oligo dT primers from Verso cDNA synthesis kit, ThermoFisher Scientific Inc. The reaction for qPCR contained ~6 ng of cDNA sample along with TB Green Premix Ex Taq II (Tli RNase H Plus) from Takara Bio Inc., and qRT-PCR was performed on the Applied Biosystems StepOne Real-Time PCR system. Gene-specific primer pairs were designed using Primer 3 software and are given in **Table 2.1**. The primer specificity is shown on gel electrophoresis, see Appendix A2.1. *RACK1* was used as a housekeeping gene and primers for *DGAT* and *RACK1* were used as already reported (Lv et al., 2013). All the experiments were performed in triplicates to check reproducibility and fold change ($\mathbf{2^{-\Delta\Delta C_T}}$) was calculated as given in

Equations 2.7 & 2.8, where C_T is the cycle threshold of the sample. The representative amplification plots and the melt curves are shown in Appendix A2.2 and A2.3.

3.3.9 Statistical analysis

The reported values were derived from an average of three independent biological replicates, and the errors represent the standard deviation (S.D.). Statistical significance of the data was obtained by Student's t-test analysis performed in MS Excel, where the data was considered significant only if $p \leq 0.05$. The maximum significance of the data was obtained with $p \leq 0.0001$.

3.4 Results

3.4.1 Effect of sodium acetate concentration and mode of cultivation on hetero/mixotrophic growth of *C. reinhardtii*

Sodium acetate (NaAc) was used as an external organic carbon source in both heterotrophic and mixotrophic modes of cultivation. To examine the effect of NaAc in the single-stage method, NaAc was added in three concentrations, i.e., 1 g/L (SS_M 1 gL^{-1}, SS_H 1 gL^{-1}), 5 g/L (SS_M 5 gL^{-1}, SS_H 5 gL^{-1}) and 10 g/L (SS_M 10 gL^{-1}, SS_H 10 gL^{-1}). An additional strategy was employed where NaAc was added in gradient mode to achieve a final concentration of 5 g/L (G_M 5 gL^{-1}, G_H 0.5_10, G_H 1_10, and G_H 1_5) as described in section 3.3.2 and **Figure 3.1**. An autotrophic control was used as the reference. **Figure 3.3** shows the growth curves for the various treatments. The growth parameters were acquired by fitting the curves as explained in section 3.3.3 and are summarized in

Table 3.1.

A prolonged lag time was observed with an increase in the acetate concentration in both heterotrophy and mixotrophic growth, compared to the autotrophic control. Interestingly, both SS_H 10 gL^{-1} and SS_M 10 gL^{-1} showed the longest lag time of 9.49 days. Under mixotrophy, SS_M 10 gL^{-1} entered the stationary phase at ~18th day, in contrast to the 8th day in other cultures. Therefore, the growth of SS_M 10 gL^{-1} was monitored for a longer period of 21 days as compared to 15 days for the rest of the

cultures. In the case of heterotrophy, the stationary phase commences variably in all conditions. While SS_H 10 gL^{-1} makes the late entry into the stationary phase on ~ the 20th day, gradient cultivations enter on the 12th day, in contrast to the 8th day in SS_H 5 gL^{-1} and the 10th day in SS_H 1 gL^{-1}. The gradient mode (G_M 5 gL^{-1}) reduced the lag time by 6 h compared to the single-stage (SS_M 5 gL^{-1}) mode in mixotrophy and an increase in the lag time was observed in heterotrophic gradient cultures. Majorly, between heterotrophy and mixotrophy, the latter showed a reduced lag time of growth. Thus, heterotrophy induces slow growth in the microalgal culture than mixotrophy. Further, SS_M 1 gL^{-1} showed no significant change in specific growth rate (μ) and doubling time (DT) compared to the autotrophy control, while SS_M 10 gL^{-1} resulted in the lowest μ of 1.04 ± 0.002 day^{-1} and highest DT of 0.67 days (16.1 h). On the other hand, SS_M 5 gL^{-1} and G_M 5 gL^{-1} exhibit the highest μ of ~3.44 ± 0.02 day^{-1} and lowest DT of 0.2 days, which is ~2.8-fold higher than the autotrophy control. Similarly, the heterotrophic cultivation showed no significant difference in the μ and DT values between the single-stage and all the gradient modes of cultivation. The change in the step size of NaAc addition causes no significant impact on the growth rate of *C. reinhardtii*. These results suggest that changing the mode of cultivation from single-stage to gradient does not alter the microalgal growth rate. G_H 1_5 possesses the highest μ of 1.33 ± 0.005 day^{-1} and the lowest DT of 0.52 days. SS_H 10 gL^{-1} shows the lowest μ of 0.20 ± 0.0004 day^{-1} and the highest DT of 3.47 days. Mixotrophic culture with 5 g/L NaAc showed the highest growth rate, and heterotrophic culture with 10 g/L NaAc showed the lowest.

NaAc concentration in both heterotrophy and mixotrophy was observed to greatly influence the growth kinetics. The optimum concentration with the highest cell density of 0.71 ± 0.01 million cells/mL was found to be 5 g/L (G_M 5 gL^{-1}) at the end of the cultivation period of 15 days. This is 1.33-fold higher than the cell density obtained in SS_M 5 gL^{-1} and 3.61-fold compared to the cell density of the autotrophy control. In comparison, SS_M 10 gL^{-1} yielded only 0.53 ± 0.01 million cells/mL at the end of 21 days of cultivation. The highest cell density yield in heterotrophy was obtained in G_H 1_10 with 0.41 ± 0.04 million cells/mL which is 1.28-fold higher than the single-stage, SS_H 5 gL^{-1}. The lowest cell density production was obtained in SS_H 1 gL^{-1} with 0.15 ± 0.02 million cells/mL, which is 1.3-fold lesser than the autotrophic control. Overall, heterotrophy resulted in poor cell density than mixotrophy.

Hence, while single-stage cultivation with 10 g/L NaAc is the least favorable for both heterotrophic and mixotrophic *Chlamydomonas reinhardtii* growth, the mixotrophic gradient cultivation with 5 g/L NaAc is the most favorable.

Table 3.1. Growth parameters and cell density yield of *C. reinhardtii* grown under hetero/mixotrophy

	Lag time (days)	Specific growth rate, μ (day^{-1})	Doubling time (days)	Cell density (Million cells/mL)
Autotrophy	1.22	1.22 ± 0.01	0.57	0.18 ± 0.01[#]
Mixotrophic cultivation				
SS_M 1 gL^{-1}	1.89	1.27 ± 0.004	0.54	0.24 ± 0.03[#]
SS_M 5 gL^{-1}	5.20	3.44 ± 0.02	0.20	0.55 ± 0.002[#]
SS_M 10 gL^{-1}	9.49	1.04 ± 0.002	0.67	0.53 ± 0.01*
G_M 5 gL^{-1}	4.95	3.45 ± 0.01	0.20	0.71 ± 0.01[#]
Heterotrophic cultivation				
SS_H 1 gL^{-1}	4.14	0.52 ± 0.006	1.33	0.15 ± 0.02[#]
SS_H 5 gL^{-1}	4.87	1.23 ± 0.005	0.56	0.32 ± 0.02[#]
SS_H 10 gL^{-1}	9.49	0.20 ± 0.0004	3.47	0.16 ± 0.01**
G_H 0.5_10	7.64	1.28 ± 0.004	0.54	0.39 ± 0.01[#]
G_H 1_10	5.56	0.95 ± 0.006	0.73	0.41 ± 0.04[#]
G_H 1_5	6.83	1.33 ± 0.005	0.52	0.39 ± 0.01[#]

[#]Cell density at the end of 15 days of cultivation, *cell density at the end of 21 days, **cell density at the end of 25 days

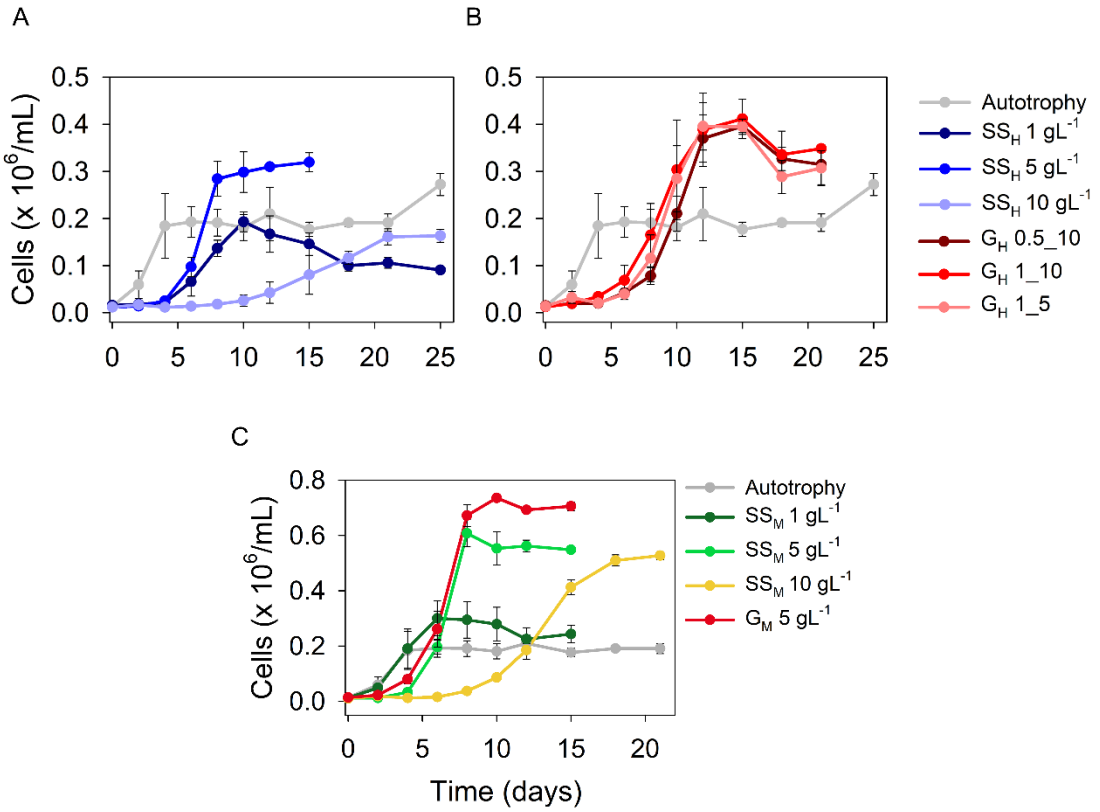

Figure 3.3. Cell density accumulation in *C. reinhardtii* culture under single-stage and gradient mode of hetero/mixotrophic cultivation.

Cell density (million cells per mL) of *C. reinhardtii* culture is represented under single-stage heterotrophic cultivation (**A**), gradient heterotrophic cultivation (**B**), and single-stage and gradient mixotrophic cultivation (**C**). The experimental conditions are the same as explained in **Figure 3.1**. Each data point in the growth curve represents the average value, and the error bars are the SDs obtained from three independent biological replicates.

3.4.2 Chlorophyll and carotenoid production in *C. reinhardtii* under hetero/mixotrophy

Photosynthetic pigments i.e., chlorophyll and carotenoids, were extracted from *C. reinhardtii* culture using 95% ethanol and estimated spectrophotometrically, (as described in the Methods section) as a function of the growth phase under hetero/mixotrophy. In heterotrophic cultivation, a significant reduction in the total chlorophyll and carotenoid content was observed, irrespective of the acetate concentration and the mode of cultivation (**Figure 3.4**). Only G_H 1_5 showed a marked increase in the carotenoid yield on day 15 of growth, with a total production of 3.53 ± 0.19 mg/mL. This was the maximum carotenoid production obtained from the heterotrophically grown cultures. Under mixotrophy, on the other hand, the net production of pigments was observed to vary with acetate concentrations and mode of cultivation (**Figure 3.5**). First of all, SS_M 1 gL^{-1} showed negligible change in the total pigment content obtained per million cells, while SS_M 5 gL^{-1} and SS_M 10 gL^{-1} produced significantly reduced pigments when the cultures were in the log phase i.e., on days 4 and 6. The pigment concentration produced by SS_M 5 gL^{-1} was lower than G_M 5 gL^{-1} by 1.2 to 2.9-fold in the case of chlorophylls and 2.2 to 2.8-fold in carotenoids (**Figure 3.5**). The cellular pigment concentration was found to increase during the stationary phase. With this regard, SS_M 10 gL^{-1} showed an accelerated production of pigments from day 15 onwards (**Figure 3.5**). On the other hand, the content in other growth conditions enhanced after day 10. Overall, the net production of these pigments was maximum at the post-stationary phase. Finally, G_M 5 gL^{-1} resulted in the highest yield of chlorophyll and carotenoids, i.e., 36.17 ± 1.74 mg/L and 8.85 ± 0.52 mg/mL, respectively. While the chlorophyll production was 3.1-fold higher than the autotrophy control, the production of carotenoids was enhanced by 3.4-fold in gradient mode. Thus, gradient cultivation not only improves cellular pigment accumulation but also benefits the large-scale production of these pigments from *C. reinhardtii* when grown mixotrophically with sodium acetate. Heterotrophic cultivation yields poor pigment content due to a lack of photosynthetic light reaction and hence becomes non-beneficial for pigment-derived phytochemical production.

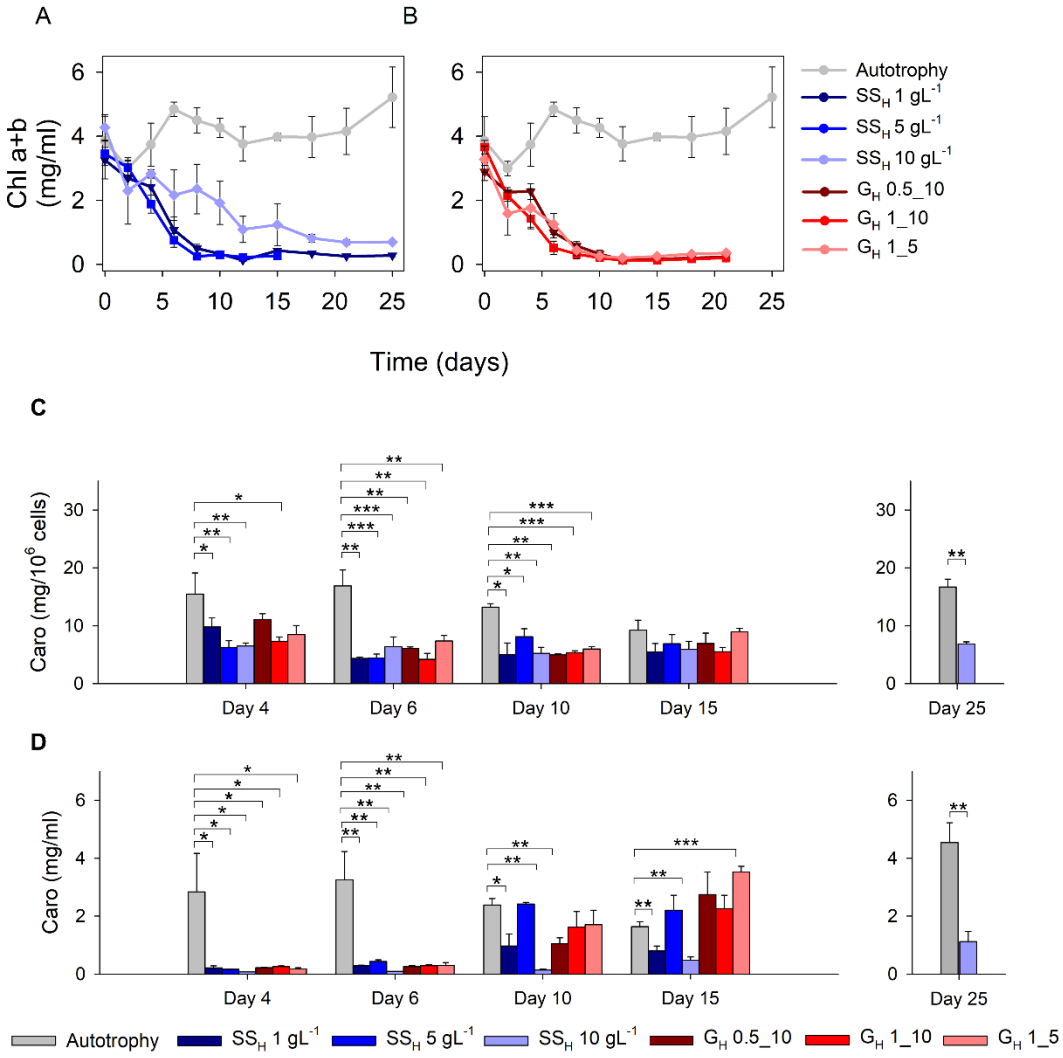

Figure 3.4. Chlorophyll and carotenoid production in *C. reinhardtii* at different stages of the growth phase when grown heterotrophically in presence of sodium acetate.

A. Total chlorophyll, Chl a+b, produced in mg per 10^6 cells with time under single-stage heterotrophy, **B.** Total chlorophyll, Chl a+b, produced in mg per 10^6 cells along the course of time under gradient heterotrophy, **C.** Carotenoids denoted in mg per 10^6 cells. **D.** Carotenoids obtained in mg/mL represent the yield. Legends for growth conditions are shown below the graphs. Error bars represent standard deviation for n = 3. *p ≤ 0.5, **p ≤ 0.01, ***p ≤ 0.001, ****p ≤ 0.0001. Significance increases as the p-value decreases.

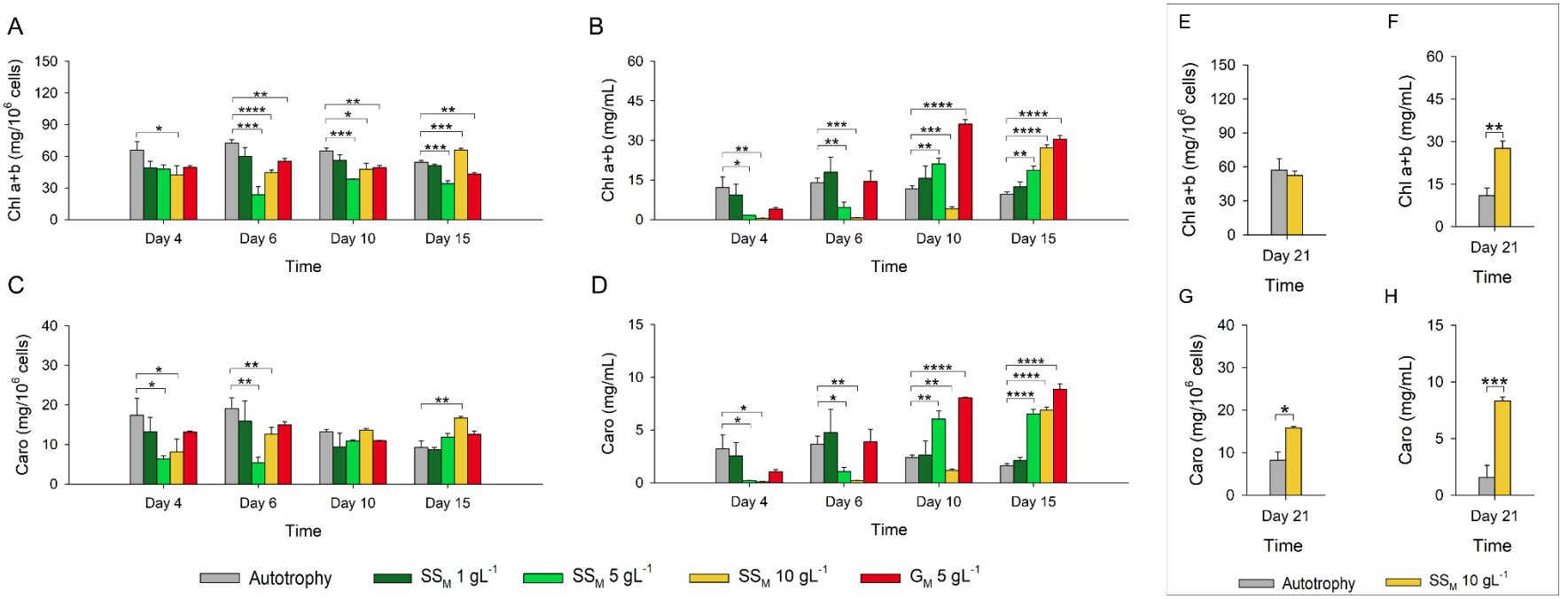

Figure 3.5. Photosynthetic pigment accumulation in *C. reinhardtii* at different stages of the growth phase when grown mixotrophically in presence of sodium acetate.

A. Total chlorophyll, Chl a+b, produced in mg per 10^6 cells. **B**. Total chlorophyll, Chl a+b produced in mg/mL representing the yield. **C**. Carotenoids denoted in mg per 10^6 cells. **D**. Carotenoids obtained in mg/mL represent the yield. **E-H.** Chlorophyll and carotenoid production on day 21. Legends for growth conditions are shown below the graphs. Error bars represent standard deviation for n = 3. *p ≤ 0.5, **p ≤ 0.01, ***p ≤ 0.001, ****p ≤ 0.0001. Significance increases as the p-value decreases.

3.4.3 Starch and lipid production in *C. reinhardtii* under hetero/mixotrophy

Starch and triacylglycerol are the reserve sources of carbon for microalgae and aid in survival during extreme environmental conditions. In the present study, heterotrophic growth caused a remarkable increase in starch production under all the experimental conditions (**Figure 3.6**). A positive correlation between the starch yields was observed with the culture age and acetate concentration. The maximum starch units were determined on day 15 with 10 g/L acetate. However, here, the mode of cultivation also becomes an important regulating factor. Among single-stage cultivation, SS_H 10 gL^{-1} yields maximum starch content of 1.15 ± 0.6 a.u. /mL on the 15^{th} day of growth (exponential phase). Gradient heterotrophy markedly increases the starch production irrespective of the step size, although the highest starch content of 6.24 ± 1.2 a.u. /mL was observed in G_H 1_10 on day 15 of culture growth, which is ~69-fold higher than autotrophy and 8.7-fold higher than the corresponding single-stage, SS_H 5 gL^{-1}. The addition of NaAc in a mixotrophic mode also enhanced the starch production compared to the autotrophy control (**Figure 3.7**). An enormous 34-fold increase in starch content (a.u. /10^6 cells) was obtained in G_M 5 gL^{-1} compared to the autotrophy control. A 1.8-fold increase in starch yield was obtained in G_M 5 gL^{-1} compared to that obtained in SS_M 5 gL^{-1}. G_M 5 gL^{-1} also produced 4.1-fold higher yields of starch (a.u. /mL) in comparison to SS_M 5 gL^{-1} obtained at the end of the cultivation period of 15 days. However, the highest starch yield of 4.71 ± 0.48 a.u. /mL was obtained from SS_M 10 gL^{-1} at the end of 21 days of cultivation. These results suggest that starch production is enhanced at high acetate concentrations and depends majorly on the mode of cultivation both in the heterotrophic and mixotrophic cultivations. The heterotrophy gradient yields maximum starch on day 15.

In contrast to the cellular production of starch at the stationary phase of the culture, TAG accumulation was observed to be maximum during the logarithmic phase of growth. Here, single-stage cultivation with 5 g/L acetate showed maximum cellular accumulation of TAG on day 6 of both heterotrophy and mixotrophy growth. SS_H 5 gL^{-1} produced ~29-fold higher TAG content than the autotrophic control on day 6 (**Figure 3.6**). However, due to increased cell density in heterotrophy (**Figure 3.3**), the net yield of TAG increased further with maximum production on day 15. SS_H 5 gL^{-1} yields a maximum TAG of 285.52 ± 14.3 f.u. /mL on day 15, only marginally higher than 232.98 ± 42.4 f.u. /mL on day 6. In the case of mixotrophy, SS_M 5 gL^{-1} produced

maximum TAG, 70.8-fold higher than G_M 5 gL^{-1}, 13-fold higher than the autotrophy control and 2.6-fold more than SS_M 10 gL^{-1} (**Figure 3.7**). The highest yield of TAG in SS_M 5 gL^{-1} was observed to be 359.57 ± 47.55 f.u. /mL. Thus, mixotrophy single-stage cultivation yields maximum TAG content during the log phase of cultivation. Overall, these results signify that starch and TAG productions are mutually exclusive and temporally well-separated. The starch content varies as a function of the carbon concentrations in the environment, while TAG production is maximum only at an optimum value. Further, gradient cultivation benefits starch production, and the single-stage favors triacylglycerol accumulation under both heterotrophy and mixotrophy modes of cultivation.

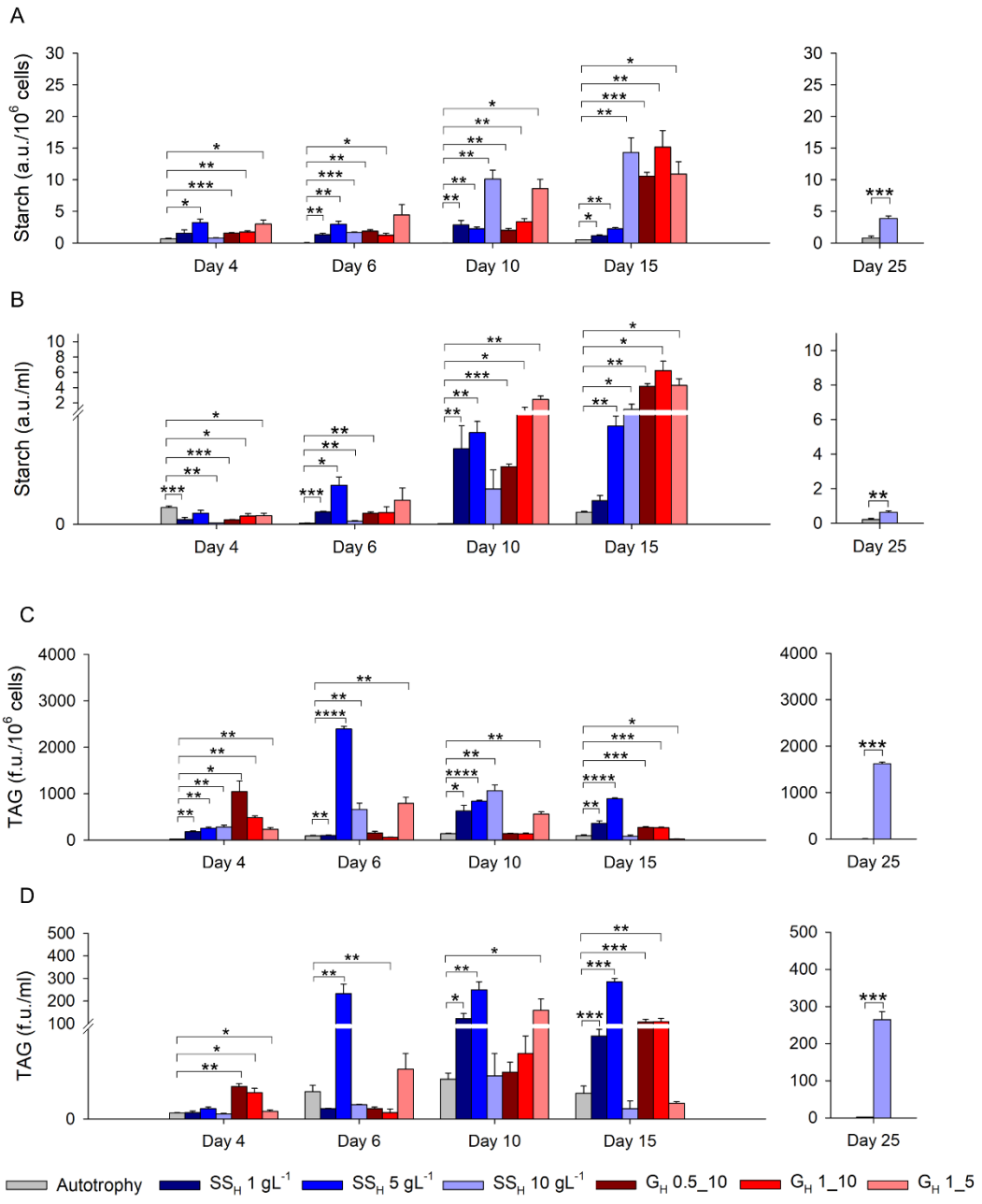

Figure 3.6. Starch and triacylglycerol production in *C. reinhardtii* at different concentrations of sodium acetate and mode of heterotrophic cultivations.

A. Starch content in absorbance units, a.u. per 10^6 cells. **B.** Total starch yield in a.u. /mL. **C.** TAG measured in fluorescence units, f.u. per 10^6 cells. **D.** TAG produced in f.u. /mL represents the yield. Legends for growth conditions are shown below the graphs. The rightmost bar chart in each panel represents the production on the 25th day of growth. Error bars represent standard deviation for n = 3. *$p \leq 0.5$, **$p \leq 0.01$, ***$p \leq 0.001$, ****$p \leq 0.0001$. Significance increases as the *p*-value decreases.

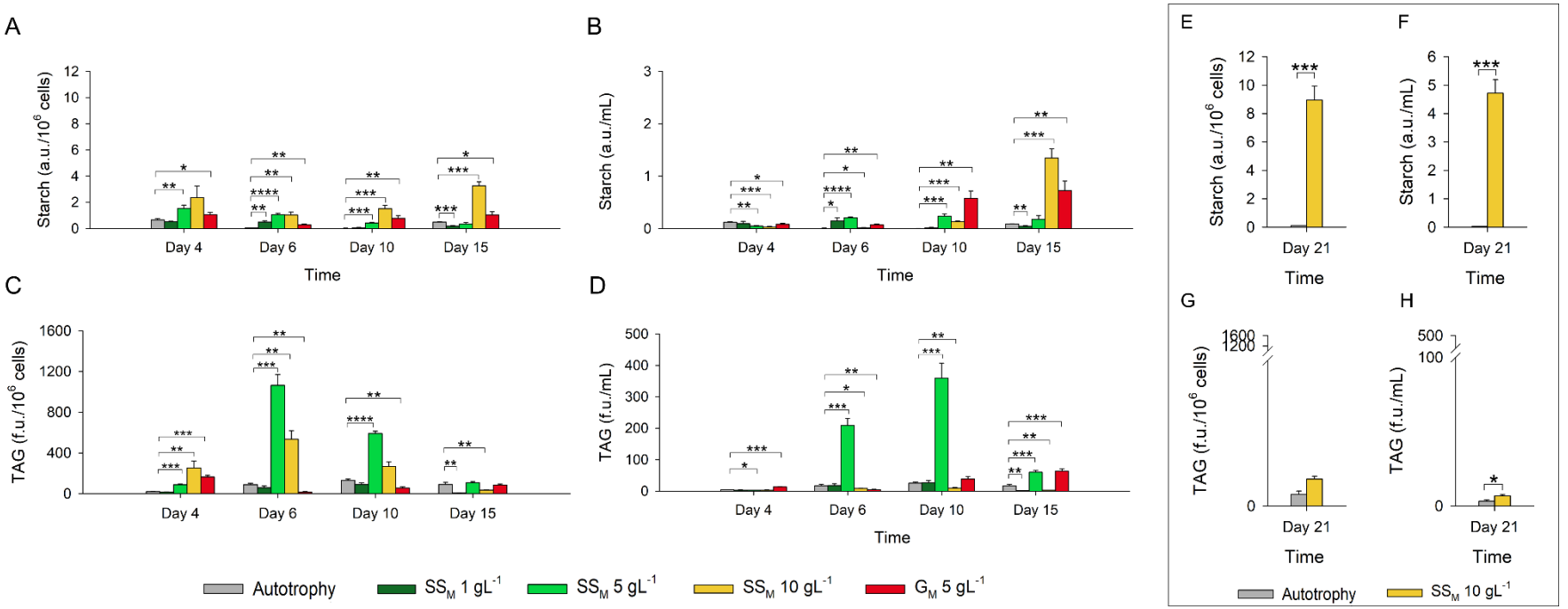

Figure 3.7. Starch and triacylglycerol accumulation in *C. reinhardtii* at different stages of growth phase under mixotrophy in presence of sodium acetate.

A. Starch content in absorbance units, a.u. per 10^6 cells. **B.** Total starch yield in a.u. /mL. **C.** TAG measured in fluorescence units, f.u. per 10^6 cells. **D.** TAG produced in f.u. /mL represents the yield. Legends for growth conditions are shown below the graphs. **E-H**. Starch and TAG production obtained on day 21 of mixotrophic cultivation. Error bars represent standard deviation for n = 3. *$p \leq 0.5$, **$p \leq 0.01$, ***$p \leq 0.001$, ****$p \leq 0.0001$. Significance increases as the *p*-value decreases

3.4.4 Study of genes affecting growth, autophagy, and lipid production in *C. reinhardtii* under mixotrophy

The biochemical analysis shows that mixotrophy yields highest cell density and lipid accumulation in *C. reinhardtii* as compared to heterotrophy and autotrophy. It, therefore, became interesting to uncover the role of metabolic genes involved in TAG production under mixotrophy cultivation with the help of gene expression study using real-time qPCR. A total of 6 genes were studied i.e., *ATG4*, *ATG8*, *DGAT*, *ACC*, *PhoA*, and *RPS6*, at the log phase (day 4) and the stationary phase (day 10) of growth. *ATG4* and *ATG8* are the autophagic genes responsible for coding AuTophaGy-related proteins, ATG4 and ATG8. Together, they assist in autophagosome formation induced by stress and result in the catabolic breakdown of membrane lipids, thereby increasing the carbon pool (M. Pérez-Pérez et al., 2017). These autophagic activities are well-known to upregulate the lipid accumulation process under oxidative stress, nutrient limitation, or heterotrophic cultivation (Kajikawa & Fukuzawa, 2020; Z. Zhang et al., 2018; Zhao et al., 2014), but only a little is known about mixotrophy (Upadhyaya & Nagar, 2018). *RPS6* codes for ribosomal protein S6, a component of the smaller ribosomal subunit, which plays a vital role in cell growth and is an indicator of autophagic flux. In this study, downregulation of *ATG4* and *ATG8* at the log phase (day 4) and upregulation at the stationary phase (day 10) in SS_M 5 gL^{-1} by 7.8 and 2.3-fold, respectively (**Figure 3.8**) are observed. These results suggest accelerated autophagy in single-stage at stationary phase. Downregulated levels of *RPS6* at day 10 in SS_M 5 gL^{-1} denote increased autophagy-induced protein degradation in single-stage. G_M 5 gL^{-1}, on the other hand, showed downregulated *ATG4* and *ATG8* expression on both days and upregulated *RPS6* expression (5.3 and 3.6-fold on day 4 and day 10, respectively) suggesting increased resistance of the microalgal cells to stress-induced autophagy in gradient mode of cultivation.

The expression of the genes responsible for lipid synthesis such as *DGAT* encoding diacylglycerol acyltransferase (DGAT) which catalyzes the acylation of the DAG molecule to form TAG, and represents the de-novo TAG synthesis (Li-Beisson et al., 2015) and *ACC* which encodes acetyl-CoA carboxylase, the rate-limiting enzyme which adds the carboxyl moiety to the acetate molecule (Johnson & Alric, 2013) was also examined. After the ACC step, the carboxy-acetylated molecule is fluxed into the de-novo fatty acid synthesis pathway. Another gene examined, *PhoA* encodes starch

phosphorylase A, which leads to starch degradation and the formation of glucose-1-phosphate (the first step in lipid synthesis). Starch-to-lipid switching is a well-known phenomenon that aids in the lipid accumulation process under stress (Ho et al., 2017). In the case of *C. reinhardtii* cells, it is observed that G_M 5 gL^{-1} induces an upregulated expression of *DGAT* and *ACC* on day 4 (3.1- fold each), which gets downregulated on day 10. *PhoA* was upregulated on both day 4 and day 10 (6.6 and 3.7-fold, respectively), however, the levels get reduced on day 10, implying a decrease in lipid production and an increase in starch formation in the stationary phase. The highest fold change was observed in the expression of genes *DGAT*, *ACC*, and *PhoA* in SS_M 5 gL^{-1}, 9.6, 35.3, and 711.2-fold, respectively (the intensity of the green color on the scale). This suggests an enhanced lipid production and starch degradation in single-stage cultivation at day 10. Overall, de-novo lipid synthesis along with carbon sequestration from starch degradation and autophagic activities were found to be highly upregulated in single-stage cultivation, accounting for the enhanced TAG accumulation. Low autophagy levels in the gradient mode of cultivation account for better cell count and reduced lag time, as noted in the Section 3.4.1.

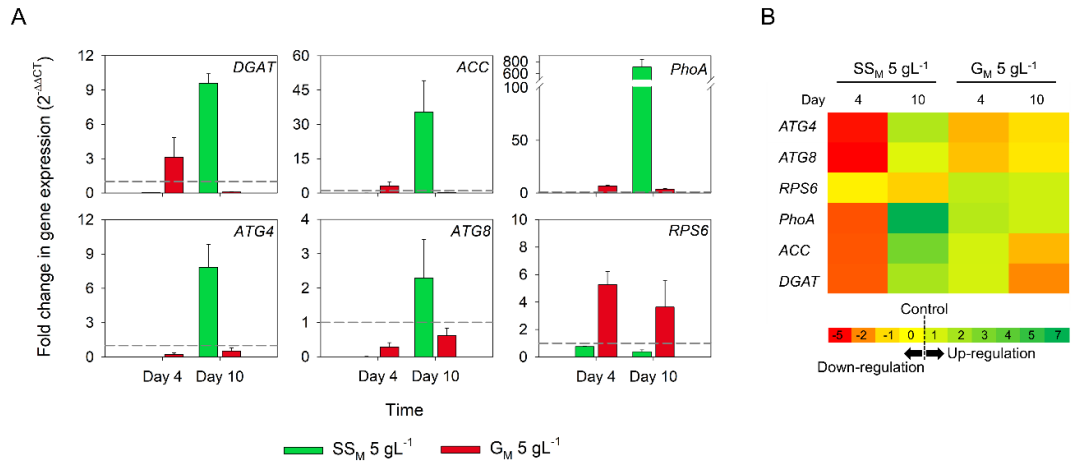

Figure 3.8. Fold change in expression of genes affecting growth, autophagy, and lipid production in *C. reinhardtii* when grown mixotrophically in presence of sodium acetate.

A. Fold change ($2^{-\Delta\Delta C_T}$) in gene expression was calculated keeping the autotrophy control as the reference, represented by a gray-colored dashed line at fold change = 1. *RACK1* is the internal control. Green bars represent SS_M 5 gL^{-1} and red bars represent G_M 5 gL^{-1}. **B.** A heat map representation of fold change (in log scale) in gene expression. The color scale at the bottom represents the natural logarithm values from lowest (red) to highest (green). Autotrophy control is represented by the dashed line at ln (1) = 0, all the values lying below 0 represent gene down-regulation and those above represent up-regulation. *DGAT*- Diacylglycerol acyltransferase, *ACC*- Acetyl-CoA carboxylase, *PhoA*- Starch phosphorylase A, *ATG4*- autophagy-related protein ATG4, *ATG8*- autophagy-related protein ATG8, *RPS6*- ribosomal protein subunit. Day 4 represents the log phase and day 10 represents the stationary phase of the culture

3.4.5 Morphological changes and lipid droplet biogenesis in *C. reinhardtii* under mixotrophy

Since mixotrophic growth results in maximum lipid production, it was interesting to observe how the lipid droplets are distributed inside these microalgal cells. The high-resolution single-cell study was performed with the single-stage mixotrophy, SS_M 5 gL^{-1}, and the corresponding gradient, G_M 5 gL^{-1} (**Figure 3.9**). The chlorophyll distribution as revealed by the bright-field microscopy indicates the presence of two kinds of cells in mixotrophy, day 6 onwards. Due to the adversity of stress, the cells begin to lose chlorophyll and appear to be bleached out. The size of the bleached population is observed more in SS_M 5 gL^{-1} than in G_M 5 gL^{-1}. The cells arrange themselves in a group of 4 cells or higher, surrounded by the palmelloid as observed in the salt stress-exposed cells (**Figures 2.14 & 2.18**). This form of organization is observed in both single-stage and gradient methods of cultivation, from day 4 onwards. The order of organization goes up to 8-celled in SS_M 5 gL^{-1} and 7-celled in G_M 5 gL^{-1}, on the 6^{th} and 10^{th} day of growth, respectively (shown by black arrows in **Figure 3.9**). Further, the cells in single-stage were observed to be non-flagellated versus the cells in gradient, for up to 6 days of growth (shown by red-colored arrow). These results suggest that single-stage imposes more adverse effects on cell morphology as compared to the gradient.

Stressful conditions lead to reactive oxygen species (ROS) production in cells, causing oxidative damage and cell death. Nutrient deficiency or salinity stress induces hypoxic conditions in a cell, increasing ROS production. Under such conditions, the liquid-liquid phase separation (LLPS) of lipid droplets (LDs) plays a major role in maintaining cellular redox and homeostasis by protecting polyunsaturated fatty acids from peroxidation-induced damage (Saito & Kimura, 2021). The effect of external carbon sources in the medium and the role it plays in influencing phase-separated LD states is largely unexplored. In this study, we examined the presence of LLPS in mixotrophic *C. reinhardtii* cells and performed the single-cell LD analysis with fluorescent microscopy. Since mixotrophic cultivation produced maximum lipid content, heterotrophic cultivation was omitted from the single-cell analysis. Remarkable differences were observed among cells grown under autotrophy, single-stage, or gradient mixotrophy (**Figure 3.10**). In the autotrophy control, there was hardly any change in the number or size of LDs and the percentage of cell area occupied by LDs (φ), as the cells progress from the log phase to the stationary phase of growth. In the

case of SS_M 5 gL^{-1}, the number, as well as the size of LDs, increase as cells age towards the stationary phase, as a result of which the LDs occupy a large volume fraction in the cell. On the other hand, enhancement in size and the number of LDs was not as pronounced in G_M 5 gL^{-1} as observed in the SS_M 5 gL^{-1} culture. A striking difference between SS_M 5 $gL^{-1}$and G_M 5 gL^{-1} was that in the former, an increase in the number of big LDs was observed, whereas, in the latter, an increase in the number of small LDs was observed during the stationary phase. In the case of SS_M 5 gL^{-1}, the cells showed growth of LDs with culture age. In G_M 5 gL^{-1}, although there was an enhancement in the number of LDs, the size of these droplets was very small. As the lipid production increased in SS_M 5 gL^{-1} culture during the stationary phase (**Figure 3.7**), the growth of LD size beyond a area fraction $\varphi_{sat} \approx 40\%$ (calculated from the phase diagram, **Figure 3.10**) facilitated complete demixing. This resulted in LD spanning almost the entire cytosolic region of the cell at the stationary phase in SS_M 5 gL^{-1} cells. To conclude, in addition to the differences in size and density of droplets, the droplet growth dynamics proceed by a different mechanism in SS_M 5 gL^{-1} cells compared to G_M 5 gL^{-1} cells.

When the area fraction occupied by the LDs in the cell, represented as φ, or the percentage area occupied by LDs, is plotted as a function of the culture age, a phase boundary could be demarcated. This boundary roughly separates the demixed state, where liquid-liquid phase separation (LLPS) was observed between the LDs and the cytosol. The phase boundary represents the coexistence of two phases in the cells or the most energetically feasible configuration for a particular area fraction. The area inside the phase boundary (blue-colored area in the **Figure 3.10D**), representing the demixed states, was more in the SS_M 5 gL^{-1} cells compared to the G_M 5 gL^{-1} cells. In autotrophy, demixed states span a tiny area fraction. The development of LLPS depends on the growth condition the cells are subjected to. Altogether, these results point towards the sensitivity of LLPS to the concentration of neutral lipids in the cells and the proteins expressed, the concentration of carbon source in the media, and the chemical components of the cytosol, which vary with the growth conditions studied here.

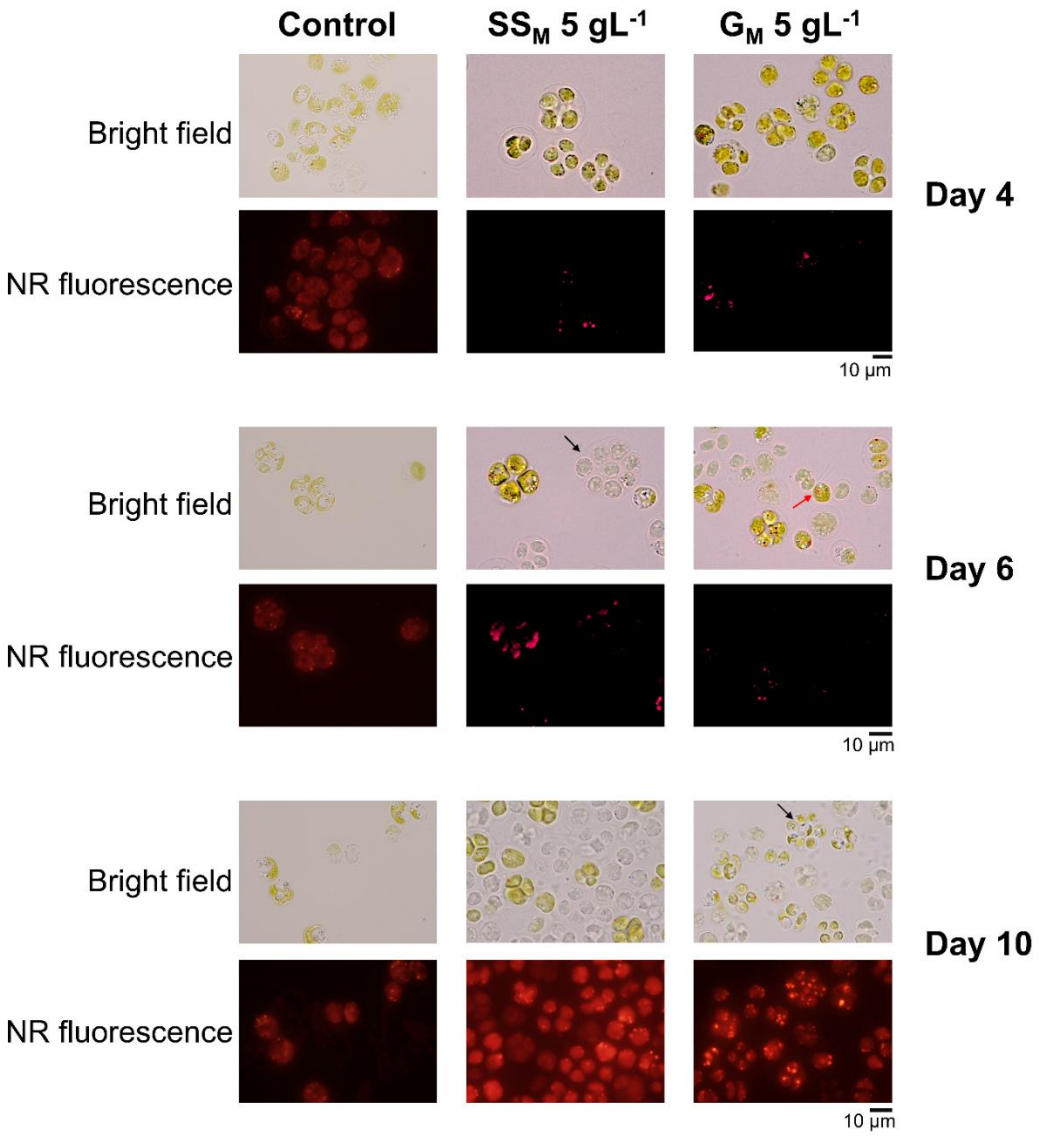

Figure 3.9. Bright field and Nile red fluorescence images showing morphological features of mixotrophic *C. reinhardtii* cells.

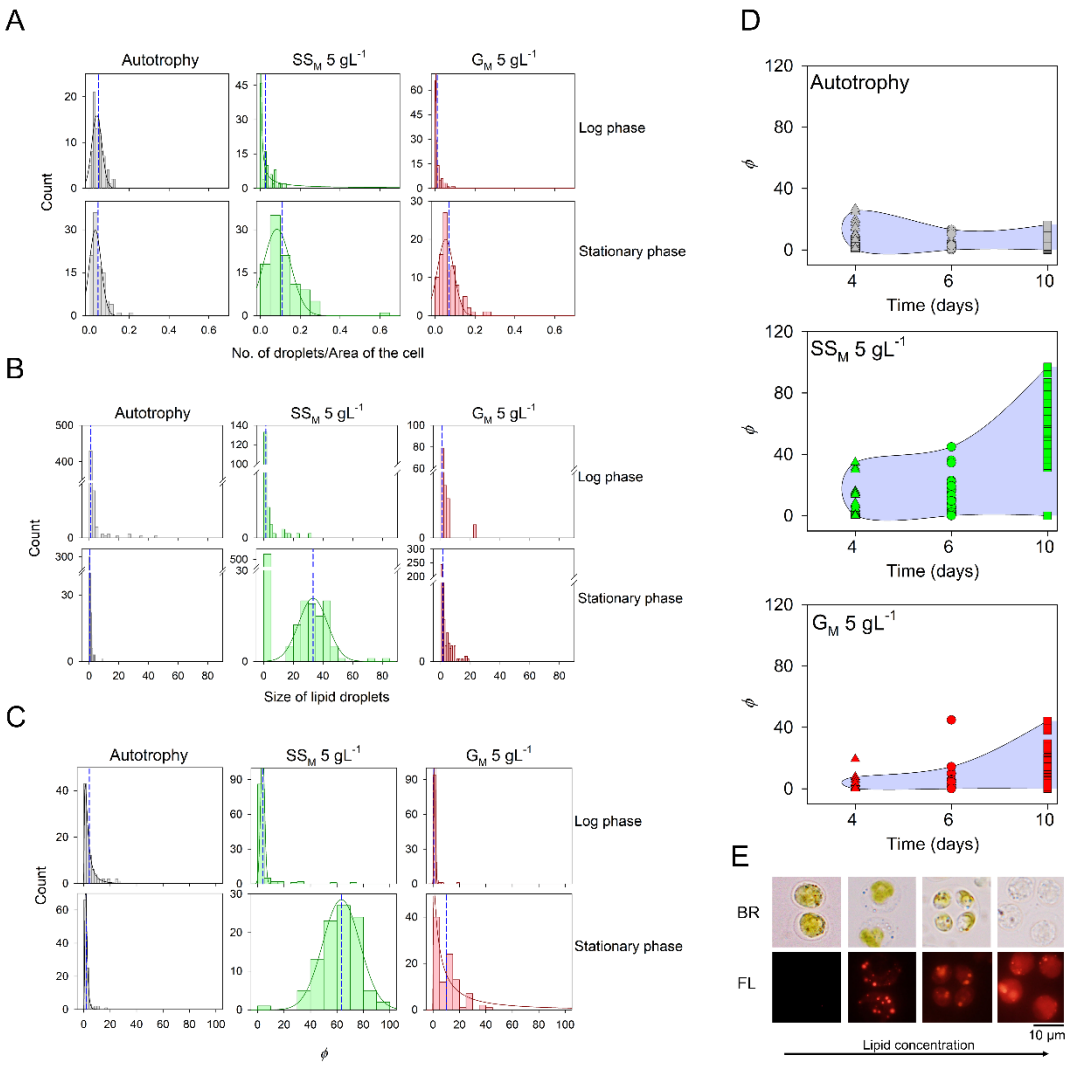

Figure 3.10. Liquid-liquid phase separation in lipid droplet biogenesis in *C. reinhardtii* under mixotrophy.

A. Lipid droplet density in SS_M 5 gL^{-1}, single-stage and G_M 5 gL^{-1}, gradient mode of cultivation compared to the autotrophy control at the log phase (day 4) and stationary phase (day 10) of growth. **B.** Dynamical changes in lipid droplet size (in μm^2) with the age of culture compared across the three growth conditions. **C.** Percentage area occupied by lipid droplets for the cell size (φ) compared across different growth conditions for the log phase and stationary growth phase. The dashed blue-colored vertical lines in panel a-c represent the population means and the curves define the distribution. **D**. Phase coexistence boundaries enclosing the coexistence of the demixed lipid droplet states with the cytosol, generated from the dependence of φ on the day of observation. Blue-colored area defines the demixed state of LDs. **E.** Representative bright-field (BR) and fluorescent (FL) microscopic images showing the progress of lipid droplet accumulation as the lipid concentration increase.

3.5 Discussion

This study focused on the differential effects imposed by the heterotrophic and mixotrophic environment on the cell density and associated production of starch and lipids by *Chlamydomonas reinhardtii*. Among the three cultivation modes, mixotrophy offers the maximum cell density output (

Table 3.1). Ge *et al.* have shown that the autotrophic-mixotrophic mode results in higher biomass productivity in *Chlorella vulgaris* than the autotrophic-heterotrophic mode (Ge et al., 2018). However, these two modes yield similar increments in the biomass content in *Chlorella protothecoides* (Heredia-Arroyo et al., 2010). Gradient administration of light, salt, or temperature stress has been shown to result in higher biomass yields in *Scenedesmus* sp., in comparison to autotrophic growth (Maneechote & Cheirsilp, 2021). This study provides new insights into biofuel production and the biomolecular mechanisms under the gradient mode of heterotrophic and mixotrophic cultivation of *C. reinhardtii.* Both heterotrophic and mixotrophic gradients with the intermediate step size (1g/L NaAc added after every 2 days) were found to enhance cell density production by ~1.3 fold as compared to their respective single-stage counterparts. The single-stage heterotrophy demotes cell density production in comparison to autotrophy. Two-stage heterotrophy in *Chlorella sorokiniana* leads to a 3.3 times higher cell density than autotrophy (Zheng et al., 2012). While the heterotrophy gradient raises the production by only 1.7-fold compared to autotrophy, mixotrophy leaps by 3.6-fold (**Table 3.1**). This is the maximum fold change obtained so far in acetate-induced mixotrophy in *C. reinhardtii*. Other studies have documented either no increase in biomass (Heifetz et al., 2000) or a minor increase of 1.1-fold in batch mixotrophy (Boyle & Morgan, 2009) and ~2-fold in fed-batch mixotrophy (Fields et al., 2018) when compared to the autotrophy control. The lag phase of the growth increases at higher sodium acetate concentrations (Bogaert et al., 2019). The acetate concentration in the medium greatly influences the growth rate of *C. reinhardtii*. 5 g/L of sodium acetate produces maximum cell density and 10 g/L results in growth inhibition. Bogaert *et al*. have recently reported maximum biomass production from *C. reinhardtii* culture when grown in presence of 5 g/L sodium acetate and 50 µmol photons m^{-2} s^{-1} light (Bogaert et al., 2019). Moon *et al.* shows that 20 g/L is the inhibiting concentration when *C. reinhardtii* is grown under a high light intensity of ~200 µmol photons m^{-2} s^{-1} (Moon et al., 2013). The light intensity used during culture growth has been shown to stimulate

acetate uptake through activities of photophosphorylation in the *Chlamydomonas* (Johnson & Alric, 2013; Smith & Gilmour, 2018). Light intensity is also a stress factor that causes oxidative stress-induced autophagy and hence retarded microalgal growth (Chouhan et al., 2022). Although there is no direct evidence of the correlation between light intensity and acetate utilization, these studies together dictate that high light decreases the tolerable acetate concentration in microalgae. Thus, light intensity becomes a crucial factor in acetate-driven microalgal growth and can be a subject of future investigations.

Acetate availability is shown to suppress photosynthesis when the mixotrophic culture is in the log phase (**Figure 3.5**). This is a well-known phenomenon observed in acetate mixotrophy when *Chlamydomonas* are grown in batch cultivation (Johnson & Alric, 2013; Roach et al., 2013; Smith & Gilmour, 2018). Puzanskiy *et al.* also illustrates that this reduction in the rate of photosynthesis occurs in the log phase of cultivation (R. K. Puzanskiy et al., 2020). In the log phase, when acetate is available in the surrounding, it is directly fluxed into the mitochondrial respiration pathway by suppressing carbon dioxide fixation in the chloroplast. This downregulates the photosynthetic pathway, not observed otherwise in the autotrophy mode (Boyle & Morgan, 2009; Chapman et al., 2015; Roach et al., 2013). According to Pang *et al.*, synergetic gaseous exchange between respiration and photosynthesis together contributes to higher biomass in mixotrophy (Pang et al., 2019). Once the carbon source is completely utilized, environmental CO_2 gets fixed by the Calvin cycle elevating the rate of photosynthesis. This explains the concomitant increase in the pigment concentration once the culture enters the stationary phase. The increase in the rate of photosynthesis after the log phase is attributed to the need for culture maintenance due to the increased cell density achieved in the culture medium (R. Puzanskiy et al., 2021). This behavior is evident in single-stage cultivation with 5 and 10 g/L acetate. In the gradient mode of cultivation, on the other hand, a gradual acclimation of the culture to the incrementing acetate concentration results in ~2.9-fold increased pigment accumulation compared to the single-stage. Since gradient cultivation produces a maximum cell density at the end of cultivation, it also generates maximum chlorophyll, 36.12 ± 1.74 mg/mL as well as carotenoids, 8.85 ± 0.52 mg/mL. The increase in the pigment yield observed in this study is higher than the one reported for fed-batch cultivation of *Chlorella* sp. FZU60, where biomass production has been shown to increase without significant impact on

the carotenoid content (Xie et al., 2019). The reduced pigment concentration observed in the heterotrophic culture is due to the lack of light-induced photosynthetic activity (**Figure 3.4**). Studies have shown that oxidative respiration contributes to the growth of heterotrophic microalgae in the presence of acetate as the metabolite (Bouarab et al., 2004). In the heterotrophic culture, the absence of light in the environment disrupts the photosynthetic activity of the cell and hence results in a significant drop in chlorophyll and carotenoid synthesis (Perez-Garcia et al., 2011). In the present study, the gradient strategy not only yields a higher cell count but also increased pigment accumulation, which can later be processed to obtain nutraceuticals and other high-value compounds.

Autophagy is known to be an effect of high light, nutrient stress, or pathogen infection (Perez-Perez et al., 2012). Interestingly, the changing modes of cultivation could also trigger autophagy in microalgae. High autophagy levels and low carotenoid content were detected in single-stage mixotrophy (**Figures 3.5 & 3.8**) suggesting an inverse relationship between the two, as observed earlier by Pérez Pérez *et al.* (M. E. Pérez-Pérez et al., 2012). This relationship is also evident in the gradient mode of cultivation, where high carotenoid accumulation results in low levels of expression of autophagy genes. Reduced autophagy under gradient cultivation justifies the good growth and increase in cell density. To the best of our knowledge, this is the first report to highlight cell density enhancement due to the lack of autophagy under gradient mixotrophic cultivation. Although there are many studies on the two-stage cultivation of other microalgae showing enhanced productivity of high-value compounds (Aziz et al., 2020; Liyanaarachchi et al., 2021; Yen & Chang, 2013), the information on gradient mixotrophy is only limited. The present study paves the way for the industrial adoption of gradient mixotrophy for the production of bioenergy feedstock.

Starch and triacylglycerol are the most commonly obtained metabolites from microalgal cultivation by biofuel industries. Starch synthesis is the default outcome of photosynthesis. Channeling acetate into the gluconeogenesis pathway leads to the production of storage carbohydrate compounds like starch (Chapman et al., 2015). In dark conditions, the assimilation of acetate by oxidative respiration increases which usually leads to storage compounds like starch (Perez-Garcia & Bashan, 2015). The present study signifies the maximum starch production under heterotrophy. Gradient heterotrophy (G_H 1_10) yields maximum starch content (**Figure 3.6**) on day 15 of growth. Acetate availability during the log phase is known to slow down the

photosynthetic pathways (J. H. Chen et al., 2021; Ran et al., 2019). As a result, starch accumulates only in the stationary phase of growth around pyrenoids in the form of granules (**Figures 3.6 & 3.7**). In mixotrophy, low expression levels of *PhoA* justify the significantly higher starch content in the gradient mode of cultivation. Furthermore, this content is also directly related to the acetate concentration. The highest amount of starch (81-fold compared to autotrophy) was obtained in the presence of 10 g/L acetate, which also produced an increased quantity of chlorophyll at the stationary phase. Cell wall-less mutant of *C. reinhardtii* has previously been shown to produce increased starch at high acetate concentrations fueled by photosynthetic reactions (Fan et al., 2012). However, the main metabolic pathways were not distinguished. Overall, a step-wise increment of acetate in a gradient strategy helps the cells to combat stress, which in the future could benefit industries producing bio feed, nutraceuticals, bioethanol, biogas, and high-value compounds.

Contrary to starch, which was obtained maximally at the stationary phase of the culture, TAG accumulation is highest at the log phase. This observation conflicts with the earlier reports claiming that TAG accumulates after starch production in the growth cycle (Fan et al., 2012; Ran et al., 2019). TAG production is highest at an optimum concentration of 5 g/L acetate (**Figures 3.6 & 3.7**). Although, increasing the acetate concentration to 80 mM from 60 mM produced an insignificant change in TAG content in *C. reinhardtii* (Fan et al., 2012). Gradient strategy did not help improve lipid production upon changing trophic modes and single-stage mixotrophy yields the highest triacylglycerol content. On the contrary, two-stage fed-batch heterotrophy in *Chlorella protothecoids* enhances lipid accumulation (T. Wang et al., 2016). A combined influence of de-novo fatty acid synthesis, TAG formation pathway, starch degradation, and autophagic flux (**Figure 3.8**) in single-stage mixotrophy together yields a ~3-fold higher content of TAG (**Figure 3.7**). The observed fold change is twice as high as the increase obtained from *C. reinhardtii* in presence of 10 g/L acetate and high light intensity (Moon et al., 2013). This makes the current method more economical and productive. Previous reports show how an increase in autophagic flux (Couso et al., 2018; Z. Zhang et al., 2018) and starch degradation in starch-less mutants drive the synthesis of lipid molecules in microalgae (Li et al., 2010; Ramanan et al., 2013). Liyanaarachchi *et al*. has summarized the phenomenon of enhanced lipid synthesis in the case of two-stage microalgal cultivation (Liyanaarachchi et al., 2021). In addition to uncovering the

advantages of gradient mixotrophy in biofuel production, this study also analyzes the metabolic pathways involved in these cultivation methods.

Chlamydomonas cells undergo palmelloid formation as a layer of protection from abiotic stress factors (Bazzani et al., 2021). An arrangement of 4-8 celled structures is a common phenomenon observed in presence of high salt concentrations i.e., 150 mM (**Figures 2.14 & 2.18**) or above (L. Y. Zhang et al., 2022) and heavy metal stress (Sabatini et al., 2011). The presence of an 8-celled structure in the present study is a unique feature observed in single-stage mixotrophy on the 6^{th} day of growth in presence of 5 g/L sodium acetate. This formation slowed down in the gradient cultivation and hence features the 7-celled organized structure on the 10^{th} day of growth (**Figure 3.9**). Loss of flagellar motility and reduction in cell size are other morphological characteristics of stress-induced microalgal cells (Boyd et al., 2017). The presence of intact flagella in the 6^{th}-day culture of gradient cultivation further signifies the leniency of carbon concentration on the cell's ability to undergo phototaxis (Boyd et al., 2017).

TAG molecules produced in single-stage mixotrophy accumulate in the form of lipid droplets (LDs) inside the cell (**Figure 3.10**). These droplets are spatially separated in the cell due to the liquid-liquid phase separation (LLPS) phenomenon. Although LLPS of LDs has been studied in various cell types (Upadhyaya & Nagar, 2018), where they are linked to various diseases, it has not been explored in microalgal cells before. The tendency of phase separation is observed in the present study to be lower in gradient mode compared to single-stage mixotrophy. The differences in the LLPS phase boundary and LD growth dynamics observed in the single-stage and gradient modes are attributed to the differential expression of regulatory proteins and lipid concentration. The enzyme involved in the final step of TAG formation, i.e., DGAT is directly linked to LD biogenesis (Walther et al., 2017). Increased TAG concentration and DGAT expression in the single-stage justify this inter-relation. The growth of LDs is regulated by a combination of thermodynamic and biological factors. LDs supposedly grow due to Ostwald ripening as a result of the coalescence of smaller droplets with bigger ones, in addition to nucleation processes (Hyman et al., 2014; Walther et al., 2017). A protein, seipin, has been observed to regulate the size of LDs in animals, plants, and fungi (Henne et al., 2020; Zoni et al., 2020). The effects of seipin have been recently studied in the microalgae, *Phaeodactylum tricornutum* (Lu et al., 2017). Simulations show that LD formation also depends on the chemical composition

of neutral lipids and the membrane curvature of the endoplasmic reticulum membrane (Zoni et al., 2020), where they are synthesized. The number of carbon atoms and unsaturation content of fatty acid defines the chemical composition of neutral lipid molecules. This composition varies from one environmental condition to another and changes biodiesel quality (Moser, 2009; Yu et al., 2011). It is, therefore, possible that droplet morphology and their physical properties can affect biodiesel quality.

LLPS of LDs is utilized by cells to deal with oxidative stress (Saito & Kimura, 2021). Since LLPS is more prominent in single-stage mixotrophic cells, it signifies that the single-stage imposes more oxidative stress on the cells compared to the gradient mode. This is also evident in the increased autophagy levels in the single stage. Overall, this part of the study highlights the necessity for a thorough investigation of the link between LLPS in microalgal cells and redox metabolism, transcriptional regulation, and signal transduction to handle oxidative stress.

In summary, while gradient heterotrophy is superior at starch production, gradient mixotrophy substantially helps in achieving the highest yields of cell density, photosynthetic pigments, and a comparative increase in starch content than the corresponding single-stage (**Figure 3.11**). Considerably low autophagy levels in gradient mixotrophy make this approach more potent in large-scale industrial production of bioenergy feedstock. High autophagy in single-stage benefits lipid production and oxidative stress causes liquid-liquid phase separation of lipid droplets, affecting their biogenesis. Thus, single-stage profits the TAG accumulation most. This previously unreported phenomenon of LLPS is observed to affect LD growth dynamics, which can cause changes in LD composition. This can potentially influence biofuel quality and open new prospects in biofuel research.

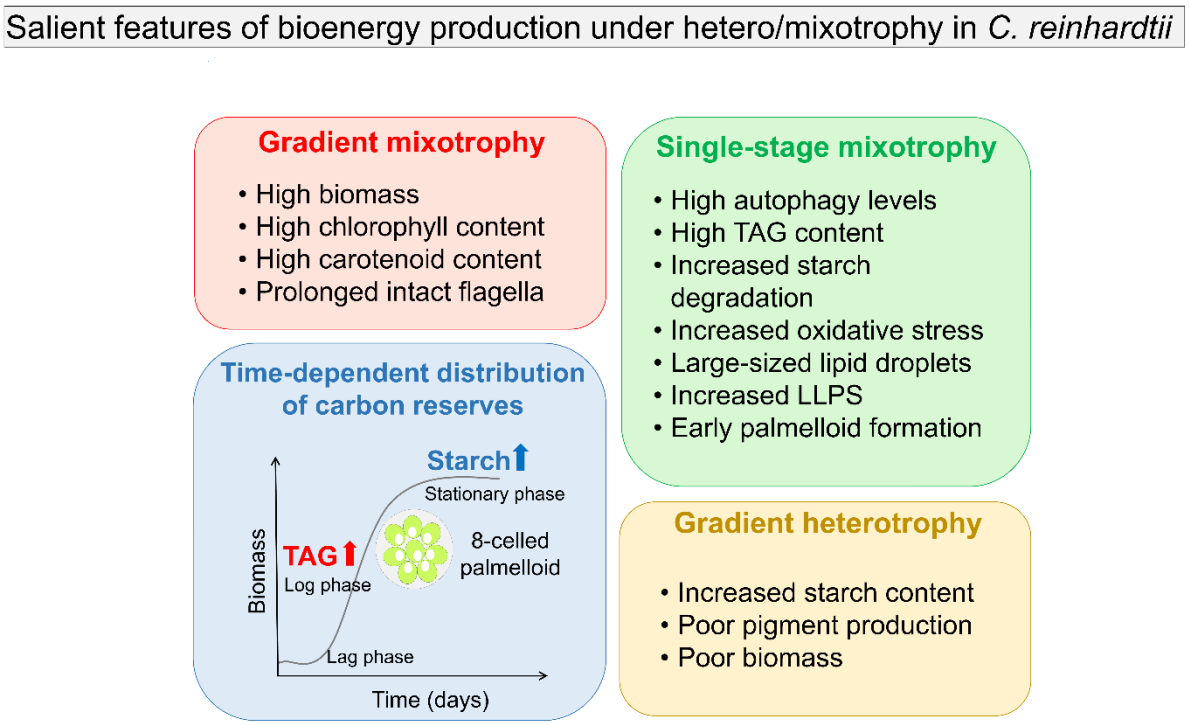

Figure 3.11. Salient features of bioenergy feedstock production in *Chlamydomonas reinhardtii* under hetero/mixotrophy.

Here, gradient mixotrophy denotes G_M 5 gL^{-1} with final sodium acetate as 5 g/L, achieved after adding 1 g/L every alternate day; single-stage mixotrophy means SS_M 5 gL^{-1} with sodium acetate as 5 g/L, achieved after adding 5 g/L at the commencement of cultivation; gradient heterotrophy denotes G_H 1_10 which is the heterotrophic analogue of G_M 5 gL^{-1} where final sodium acetate of 5 g/L is achieved after adding 1 g/L every alternate day.

3.6 Conclusion

This study presents a comparative analysis of the role of heterotrophy and mixotrophy in bioenergy feedstock production in *Chlamydomonas reinhardtii*. The gradient strategy of adding sodium acetate emerges to be the most suitable method for cultivation and metabolite production. The details of the lipid droplet morphology and growth dynamics explain the potential influence of liquid-liquid phase separation on biodiesel quality. Together, the mode of cultivation and physical characteristics of lipid droplets open new prospects in biofuel research and offer great potential for optimizations of industrial-scale production.

3.7 References

Aziz, M. M. A., Kassim, K. A., Shokravi, Z., Jakarni, F. M., Lieu, H. Y., Zaini, N., Tan, L. S., Islam, S., & Shokravi, H. (2020). Two-stage cultivation strategy for simultaneous increases in growth rate and lipid content of microalgae: A review. *Renewable and Sustainable Energy Reviews*, *119*(November 2019), 109621. https://doi.org/10.1016/j.rser.2019.109621

Bazzani, E., Lauritano, C., Mangoni, O., Bolinesi, F., & Saggiomo, M. (2021). *Chlamydomonas* responses to salinity stress and possible biotechnological exploitation. *Journal of Marine Science and Engineering*, *9*(11). https://doi.org/10.3390/jmse9111242

Bell, S. A., Shen, C., Brown, A., & Hunt, A. G. (2016). Experimental Genome-Wide Determination of RNA Polyadenylation in *Chlamydomonas reinhardtii*. https://doi.org/10.1371/journal.pone.0146107

Bhatnagar, A., Chinnasamy, S., Singh, M., & Das, K. C. (2011). Renewable biomass production by mixotrophic algae in the presence of various carbon sources and wastewaters. *Applied Energy*, *88*(10), 3425–3431. https://doi.org/10.1016/j.apenergy.2010.12.064

Black, S. K., Smolinski, S. L., Feehan, C., Pienkos, P. T., Jarvis, E. E., & Laurens, L. M. L. (2013). New method for discovery of starch phenotypes in growing microalgal colonies. *Analytical Biochemistry*, *432*(2), 71–73. https://doi.org/10.1016/j.ab.2012.09.018

Bogaert, K. A., Perez, E., Rumin, J., Giltay, A., Carone, M., Coosemans, N., Radoux, M., Eppe, G., Levine, R. D., Remacle, F., & Remacle, C. (2019). Metabolic, Physiological, and Transcriptomics Analysis of Batch Cultures of the Green Microalga *Chlamydomonas* Grown on Different Acetate Concentrations. *Cells*, *8*(11), 1–21. https://doi.org/10.3390/cells8111367

Bouarab, L., Dauta, A., & Loudiki, M. (2004). Heterotrophic and mixotrophic growth of Micractinium pusillum Fresenius in the presence of acetate and glucose:effect of light and acetate gradient concentration. *Water Research*, *38*(11), 2706–2712. https://doi.org/10.1016/j.watres.2004.03.021

Boyd, M., Rosenzweig, F., & Herron, M. (2017). Motility in multicellular *Chlamydomonas reinhardtii* (Chlamydomonadales, Chlorophyceae). *BioRxiv*, 201194. https://www.biorxiv.org/content/10.1101/201194v1%0Ahttps://www.biorxiv.org/content/10.1101/201194v1.abstract

Boyle, N. R., & Morgan, J. A. (2009). Flux balance analysis of primary metabolism in *Chlamydomonas reinhardtii*. *BMC Systems Biology*, *3*, 1–14. https://doi.org/10.1186/1752-0509-3-4

Cai, M., Shi, R., Huang, S., & Qi, A. (2008). Comparison of mixotrophic and hotoautotrophic growth of *Haematococcus pluvialis* for astaxanthin production. *Journal of Biotechnology*, *136*, S575–S576. https://doi.org/10.1016/J.JBIOTEC.2008.07.1357

Cakmak, T., Angun, P., Demiray, Y. E., Ozkan, A. D., Elibol, Z., & Tekinay, T. (2012). Differential effects of nitrogen and sulfur deprivation on growth and biodiesel feedstock production of *Chlamydomonas reinhardtii*. *Biotechnology and Bioengineering*, *109*(8), 1947–1957. https://doi.org/10.1002/bit.24474

Chapman, S. P., Paget, C. M., Johnson, G. N., & Schwartz, J. M. (2015). Flux balance analysis reveals acetate metabolism modulates cyclic electron flow and alternative glycolytic pathways in *Chlamydomonas reinhardtii*. *Frontiers in Plant Science*, *6*(JUNE), 1–14. https://doi.org/10.3389/fpls.2015.00474

Chen, C. Y., & Liu, C. C. (2018). Optimization of lutein production with a two-stage

mixotrophic cultivation system with *Chlorella sorokiniana* MB-1. *Bioresource Technology*, *262*(April), 74–79. https://doi.org/10.1016/j.biortech.2018.04.024

Chen, J. H., Kato, Y., Matsuda, M., Chen, C. Y., Nagarajan, D., Hasunuma, T., Kondo, A., & Chang, J. S. (2021). Lutein production with *Chlorella sorokiniana* MB-1-M12 using novel two-stage cultivation strategies – metabolic analysis and process improvement. *Bioresource Technology*, *334*(April), 125200. https://doi.org/10.1016/j.biortech.2021.125200

Chen, W., Zhang, C., Song, L., Sommerfeld, M., & Hu, Q. (2009). A high throughput Nile red method for quantitative measurement of neutral lipids in microalgae. *Journal of Microbiological Methods*, *77*(1), 41–47. https://doi.org/10.1016/j.mimet.2009.01.001

Chouhan, N., Devadasu, E., Yadav, R. M., & Subramanyam, R. (2022). Autophagy Induced Accumulation of Lipids in pgrl1 and pgr5 of *Chlamydomonas reinhardtii* Under High Light. *Frontiers in Plant Science*, *12*(January). https://doi.org/10.3389/fpls.2021.752634

Couso, I., Pérez-Pérez, M. E., Martínez-Force, E., Kim, H. S., He, Y., Umen, J. G., & Crespo, J. L. (2018). Autophagic flux is required for the synthesis of triacylglycerols and ribosomal protein turnover in *Chlamydomonas*. *Journal of Experimental Botany*, *69*(6), 1355–1367. https://doi.org/10.1093/jxb/erx372

da Silva, T. L., Moniz, P., Silva, C., & Reis, A. (2021). The role of heterotrophic microalgae in waste conversion to biofuels and bioproducts. *Processes*, *9*(7), 1–24. https://doi.org/10.3390/pr9071090

Fan, J., Yan, C., Andre, C., Shanklin, J., Schwender, J., & Xu, C. (2012). Oil accumulation is controlled by carbon precursor supply for fatty acid synthesis in *Chlamydomonas reinhardtii*. *Plant and Cell Physiology*, *53*(8), 1380–1390. https://doi.org/10.1093/pcp/pcs082

Fields, F. J., Ostrand, J. T., & Mayfield, S. P. (2018). Fed-batch mixotrophic cultivation of *Chlamydomonas reinhardtii* for high-density cultures. *Algal Research*, *33*(March 2017), 109–117. https://doi.org/10.1016/j.algal.2018.05.006

Ge, S., Qiu, S., Tremblay, D., Viner, K., Champagne, P., & Jessop, P. G. (2018). Centrate wastewater treatment with *Chlorella vulgaris*: Simultaneous enhancement of nutrient removal, biomass and lipid production. *Chemical Engineering Journal*, *342*, 310–320. https://doi.org/10.1016/j.cej.2018.02.058

Goncalves, E. C., Wilkie, A. C., Kirst, M., & Rathinasabapathi, B. (2016). Metabolic regulation of triacylglycerol accumulation in the green algae: identification of potential targets for engineering to improve oil yield. *Plant Biotechnology Journal*, *14*(8), 1649–1660. https://doi.org/10.1111/pbi.12523

Harris, E. H. (2001). *Chlamydomonas* As a Model Organism. *Annu. Rev. Plant Physiol. Plant Mol. Biol*, *52*, 363–406. https://doi.org/10.1146/annurev.arplant.52.1.363

Heifetz, P. B., Förster, B., Osmond, C. B., Giles, L. J., & Boynton, J. E. (2000). Effects of acetate on facultative autotrophy in *Chlamydomonas reinhardtii* assessed by photosynthetic measurements and stable isotope analyses. *Plant Physiology*, *122*(4), 1439–1445. https://doi.org/10.1104/pp.122.4.1439

Henne, M., Goodman, J. M., & Hariri, H. (2020). Spatial compartmentalization of lipid droplet biogenesis. *Biochimica et Biophysica Acta - Molecular and Cell Biology of Lipids*, *1865*(1), 158499. https://doi.org/10.1016/j.bbalip.2019.07.008

Heredia-Arroyo, T., Wei, W., & Hu, B. (2010). Oil accumulation via heterotrophic/mixotrophic *Chlorella protothecoides*. *Applied Biochemistry and Biotechnology*, *162*(7), 1978–1995.

https://doi.org/10.1007/s12010-010-8974-4

Ho, S. H., Nakanishi, A., Kato, Y., Yamasaki, H., Chang, J. S., Misawa, N., Hirose, Y., Minagawa, J., Hasunuma, T., & Kondo, A. (2017). Dynamic metabolic profiling together with transcription analysis reveals salinity-induced starch-To-lipid biosynthesis in alga *Chlamydomonas* sp. JSC4. *Scientific Reports*, *7*(April), 1–7. https://doi.org/10.1038/srep45471

Hyman, A. A., Weber, C. A., & Jülicher, F. (2014). Liquid-liquid phase separation in biology. *Annual Review of Cell and Developmental Biology*, *30*, 39–58. https://doi.org/10.1146/annurev-cellbio-100913-013325

Jin, H., Zhang, H., Zhou, Z., Li, K., Hou, G., Xu, Q., Chuai, W., Zhang, C., Han, D., & Hu, Q. (2020). Ultrahigh-cell-density heterotrophic cultivation of the unicellular green microalga *Scenedesmus acuminatus* and application of the cells to photoautotrophic culture enhance biomass and lipid production. *Biotechnology and Bioengineering*, *117*(1), 96–108. https://doi.org/10.1002/bit.27190

Johnson, X., & Alric, J. (2013). Central carbon metabolism and electron transport in *Chlamydomonas reinhardtii*: Metabolic constraints for carbon partitioning between oil and starch. *Eukaryotic Cell*, *12*(6), 776–793. https://doi.org/10.1128/EC.00318-12

Kajikawa, M., & Fukuzawa, H. (2020). Algal Autophagy Is Necessary for the Regulation of Carbon Metabolism Under Nutrient Deficiency. *Frontiers in Plant Science*, *11*(February), 1–6. https://doi.org/10.3389/fpls.2020.00036

Khan, M. U., & Mitchell, K. (1987). Chlorophylls Carotenoids. *Methods in Enzymology*, *148*, 350–382.

Kim, H. S., Guzman, A. R., Thapa, H. R., Devarenne, T. P., & Han, A. (2016). A droplet microfluidics platform for rapid microalgal growth and oil production analysis. *Biotechnology and Bioengineering*, *113*(8), 1691–1701. https://doi.org/10.1002/bit.25930

Kim, S., Park, J. eun, Cho, Y. B., & Hwang, S. J. (2013). Growth rate, organic carbon and nutrient removal rates of *Chlorella sorokiniana* in autotrophic, heterotrophic and mixotrophic conditions. *Bioresource Technology*, *144*, 8–13. https://doi.org/10.1016/j.biortech.2013.06.068

Kou, Z., Bei, S., Sun, J., & Pan, J. (2013). Fluorescent measurement of lipid content in the model organism *Chlamydomonas reinhardtii*. *Journal of Applied Phycology*, *25*(6), 1633–1641. https://doi.org/10.1007/s10811-013-0011-x

Li-Beisson, Y., Beisson, F., & Riekhof, W. (2015). Metabolism of acyl-lipids in *Chlamydomonas reinhardtii*. *Plant Journal*, *82*(3), 504–522. https://doi.org/10.1111/tpj.12787

Li-Beisson, Y., Kong, F., Wang, P., Lee, Y., & Kang, B. H. (2021). The disassembly of lipid droplets in *Chlamydomonas*. *New Phytologist*, *231*(4), 1359–1364. https://doi.org/10.1111/nph.17505

Li, Y., Han, D., Hu, G., Sommerfeld, M., & Hu, Q. (2010). Inhibition of starch synthesis results in overproduction of lipids in *Chlamydomonas reinhardtii*. *Biotechnology and Bioengineering*, *107*(2), 258–268. https://doi.org/10.1002/bit.22807

Lin, T. S., & Wu, J. Y. (2015). Effect of carbon sources on growth and lipid accumulation of newly isolated microalgae cultured under mixotrophic condition. *Bioresource Technology*, *184*, 100–107. https://doi.org/10.1016/j.biortech.2014.11.005

Liyanaarachchi, V. C., Premaratne, M., Ariyadasa, T. U., Nimarshana, P. H. V., & Malik, A. (2021). Two-stage cultivation of microalgae for production of high-value compounds and

biofuels: A review. *Algal Research*, *57*(May), 102353. https://doi.org/10.1016/j.algal.2021.102353

Lowrey, J., Brooks, M. S., & McGinn, P. J. (2015). Heterotrophic and mixotrophic cultivation of microalgae for biodiesel production in agricultural wastewaters and associated challenges—a critical review. *Journal of Applied Phycology*, *27*(4), 1485–1498. https://doi.org/10.1007/s10811-014-0459-3

Lu, Y., Wang, X., Balamurugan, S., Yang, W. D., Liu, J. S., Dong, H. P., & Li, H. Y. (2017). Identification of a putative seipin ortholog involved in lipid accumulation in marine microalga *Phaeodactylum tricornutum*. *Journal of Applied Phycology*, *29*(6), 2821–2829. https://doi.org/10.1007/s10811-017-1173-8

Lv, H., Qu, G., Qi, X., Lu, L., Tian, C., & Ma, Y. (2013). Transcriptome analysis of *Chlamydomonas reinhardtii* during the process of lipid accumulation. *Genomics*, *101*(4), 229–237. https://doi.org/10.1016/j.ygeno.2013.01.004

Ma, R., Zhang, Z., Ho, S. H., Ruan, C., Li, J., Xie, Y., Shi, X., Liu, L., & Chen, J. (2020). Two-stage bioprocess for hyper-production of lutein from microalga *Chlorella sorokiniana* FZU60: Effects of temperature, light intensity, and operation strategies. *Algal Research*, *52*(November), 102119. https://doi.org/10.1016/j.algal.2020.102119

Maneechote, W., & Cheirsilp, B. (2021). Stepwise-incremental physicochemical factors induced acclimation and tolerance in oleaginous microalgae to crucial outdoor stresses and improved properties as biodiesel feedstocks. *Bioresource Technology*, *328*(December 2020), 124850. https://doi.org/10.1016/j.biortech.2021.124850

Miao, X., & Wu, Q. (2006). Biodiesel production from heterotrophic microalgal oil. *Bioresource Technology*, *97*(6), 841–846. https://doi.org/10.1016/j.biortech.2005.04.008

Moon, M., Kim, C. W., Park, W. K., Yoo, G., Choi, Y. E., & Yang, J. W. (2013). Mixotrophic growth with acetate or volatile fatty acids maximizes growth and lipid production in *Chlamydomonas reinhardtii*. *Algal Research*, *2*(4), 352–357. https://doi.org/10.1016/j.algal.2013.09.003

Moser, B. R. (2009). Biodiesel production, properties, and feedstocks. *In Vitro Cellular & Developmental Biology - Plant*, *45*(3), 229–266. https://doi.org/10.1007/s11627-009-9204-z

Msanne, J., Polle, J., & Starkenburg, S. (2020). An assessment of heterotrophy and mixotrophy in *Scenedesmus* and its utilization in wastewater treatment. *Algal Research*, *48*(January), 101911. https://doi.org/10.1016/j.algal.2020.101911

Nicodemou, A., Kallis, M., Agapiou, A., Markidou, A., & Koutinas, M. (2022). The Effect of Trophic Modes on Biomass and Lipid Production of Five Microalgal Strains. *Water (Switzerland)*, *14*(2), 1–14. https://doi.org/10.3390/w14020240

Pang, N., Gu, X., Chen, S., Kirchhoff, H., Lei, H., & Roje, S. (2019). Exploiting mixotrophy for improving productivities of biomass and co-products of microalgae. *Renewable and Sustainable Energy Reviews*, *112*(June), 450–460. https://doi.org/10.1016/j.rser.2019.06.001

Park, W. K., Moon, M., Kwak, M. S., Jeon, S., Choi, G. G., Yang, J. W., & Lee, B. (2014). Use of orange peel extract for mixotrophic cultivation of *Chlorella vulgaris*: Increased production of biomass and FAMEs. *Bioresource Technology*, *171*, 343–349. https://doi.org/10.1016/j.biortech.2014.08.109

Perez-Garcia, O., & Bashan, Y. (2015). Algal biorefineries: Volume 2: Products and refinery design. In *Algal Biorefineries: Volume 2: Products and Refinery Design* (Issue January

2016). https://doi.org/10.1007/978-3-319-20200-6

Perez-Garcia, O., Escalante, F. M. E., de-Bashan, L. E., & Bashan, Y. (2011). Heterotrophic cultures of microalgae: Metabolism and potential products. *Water Research*, *45*(1), 11–36. https://doi.org/10.1016/j.watres.2010.08.037

Pérez-Pérez, M., Couso, I., Heredia-Martínez, L., & Crespo, J. (2017). Monitoring Autophagy in the Model Green Microalga *Chlamydomonas reinhardtii*. *Cells*, *6*(4), 36. https://doi.org/10.3390/cells6040036

Pérez-Pérez, M. E., Couso, I., & Crespo, J. L. (2012). Carotenoid deficiency triggers autophagy in the model green alga *Chlamydomonas reinhardtii*. *Autophagy*, *8*(3), 376–388. https://doi.org/10.4161/auto.8.3.18864

Perez-Perez, M. E., Lemaire, S. D., & Crespo, J. L. (2012). Reactive Oxygen Species and Autophagy in Plants and Algae. *Plant Physiology*, *160*(1), 156–164. https://doi.org/10.1104/pp.112.199992

Puzanskiy, R. K., Romanyuk, D. A., & Shishova, M. F. (2020). Shift in Expression of the Genes of Primary Metabolism and Chloroplast Transporters in *Chlamydomonas reinhardtii* under Different Trophic Conditions. *Russian Journal of Plant Physiology*, *67*(5), 867–878. https://doi.org/10.1134/S102144372005012X

Puzanskiy, R., Shavarda, A., Romanyuk, D., & Shishova, M. (2021). The role of trophic conditions in the regulation of physiology and metabolism of *Chlamydomonas reinhardtii* during batch culturing. *Journal of Applied Phycology*, *33*(5), 2897–2908. https://doi.org/10.1007/s10811-021-02510-3

Ramanan, R., Kim, B. H., Cho, D. H., Ko, S. R., Oh, H. M., & Kim, H. S. (2013). Lipid droplet synthesis is limited by acetate availability in starchless mutant of *Chlamydomonas reinhardtii*. *FEBS Letters*, *587*(4), 370–377. https://doi.org/10.1016/j.febslet.2012.12.020

Ran, W., Wang, H., Liu, Y., Qi, M., Xiang, Q., Yao, C., Zhang, Y., & Lan, X. (2019). Storage of starch and lipids in microalgae: Biosynthesis and manipulation by nutrients. *Bioresource Technology*, *291*(June), 121894. https://doi.org/10.1016/j.biortech.2019.121894

Roach, T., Sedoud, A., & Krieger-Liszkay, A. (2013). Acetate in mixotrophic growth medium affects photosystem II in *Chlamydomonas reinhardtii* and protects against photoinhibition. *Biochimica et Biophysica Acta - Bioenergetics*, *1827*(10), 1183–1190. https://doi.org/10.1016/j.bbabio.2013.06.004

Sabatini, S. E., Leonardi, P. I., & Rodríguez, M. C. (2011). Responses to sublethal copper exposure in two strains of *Chlamydomonas reinhardtii* (Volvocales, Chlorophyceae) in autotrophic and mixotrophic conditions. *Phycologia*, *50*(1), 78–88. https://doi.org/10.2216/09-101.1

Saito, Y., & Kimura, W. (2021). Roles of Phase Separation for Cellular Redox Maintenance. *Frontiers in Genetics*, *12*(July), 1–15. https://doi.org/10.3389/fgene.2021.691946

Singh, H., Shukla, M. R., Chary, K. V. R., & Rao, B. J. (2014). Acetate and bicarbonate assimilation and metabolite formation in *Chlamydomonas reinhardtii*: A13C-NMR study. *PLoS ONE*, *9*(9). https://doi.org/10.1371/journal.pone.0106457

Smith, R. T., & Gilmour, D. J. (2018). The influence of exogenous organic carbon assimilation and photoperiod on the carbon and lipid metabolism of *Chlamydomonas reinhardtii*. *Algal Research* (Vol. 31, pp. 122–137). https://doi.org/10.1016/j.algal.2018.01.020

Upadhyaya, S., & Nagar, N. (2018). Modulation of TOR kinase activity in *Chlamydomonas reinhardtii*: Effect of N-starvation and changing carbon pool Shivani. *BioRxiv Preprint*.

https://doi.org/10.1101/312942

Walther, T. C., Chung, J., & Farese, R. V. (2017). Lipid droplet biogenesis. *Annual Review of Cell and Developmental Biology*, *33*, 491–510. https://doi.org/10.1146/annurev-cellbio-100616-060608

Wan, M., Liu, P., Xia, J., Rosenberg, J. N., Oyler, G. A., Betenbaugh, M. J., Nie, Z., & Qiu, G. (2011). The effect of mixotrophy on microalgal growth, lipid content, and expression levels of three pathway genes in *Chlorella sorokiniana*. *Applied Microbiology and Biotechnology*, *91*(3), 835–844. https://doi.org/10.1007/s00253-011-3399-8

Wang, T., Tian, X., Liu, T., Wang, Z., Guan, W., Guo, M., Chu, J., & Zhuang, Y. (2016). Enhancement of lipid productivity with a novel two-stage heterotrophic fed-batch culture of *Chlorella protothecoides* and a trial of CO2 recycling by coupling with autotrophic process. *Biomass and Bioenergy*, *95*, 235–243. https://doi.org/10.1016/j.biombioe.2016.10.010

Wang, Y., & Peng, J. (2008). Growth-associated biosynthesis of astaxanthin in heterotrophic *Chlorella zofingiensis* (Chlorophyta). *World Journal of Microbiology and Biotechnology*, *24*(9), 1915–1922. https://doi.org/10.1007/s11274-008-9692-8

Xie, Y., Li, J., Ma, R., Ho, S. H., Shi, X., Liu, L., & Chen, J. (2019). Bioprocess operation strategies with mixotrophy/photoinduction to enhance lutein production of microalga *Chlorella sorokiniana* FZU60. *Bioresource Technology*, *290*(June), 121798. https://doi.org/10.1016/j.biortech.2019.121798

Xiong, W., Gao, C., Yan, D., Wu, C., & Wu, Q. (2010). Double CO2 fixation in photosynthesis-fermentation model enhances algal lipid synthesis for biodiesel production. *Bioresource Technology*, *101*(7), 2287–2293. https://doi.org/10.1016/j.biortech.2009.11.041

Yen, H. W., & Chang, J. T. (2013). A two-stage cultivation process for the growth enhancement of *Chlorella vulgaris*. *Bioprocess and Biosystems Engineering*, *36*(11), 1797–1801. https://doi.org/10.1007/s00449-013-0922-6

Yu, W., Ansari, W., Schoepp, N. G., Hannon, M. J., Mayfield, S. P., & Burkart, M. D. (2011). Modifications of the metabolic pathways of lipid and triacylglycerol production in microalgae. *Microbial Cell Factories*, *10*(91), 1–11.

Zhang, L. Y., Xing, Z. T., Chen, L. Q., Zhang, X. J., & Fan, S. J. (2022). Comprehensive Time-Course Transcriptome and Co-expression Network Analyses Identify Salt Stress Responding Mechanisms in *Chlamydomonas reinhardtii* Strain GY-D55. *Frontiers in Plant Science*, *13*(February), 1–17. https://doi.org/10.3389/fpls.2022.828321

Zhang, Z., Sun, D., Cheng, K. W., & Chen, F. (2018). Inhibition of autophagy modulates astaxanthin and total fatty acid biosynthesis in *Chlorella zofingiensis* under nitrogen starvation. *Bioresource Technology*, *247*(September 2017), 610–615. https://doi.org/10.1016/j.biortech.2017.09.133

Zhao, L., Dai, J., & Wu, Q. (2014). Autophagy-like processes are involved in lipid droplet degradation in *Auxenochlorella protothecoides* during the heterotrophy-autotrophy transition. *Frontiers in Plant Science*, *5*(AUG), 1–12. https://doi.org/10.3389/fpls.2014.00400

Zheng, Y., Chi, Z., Lucker, B., & Chen, S. (2012). Two-stage heterotrophic and phototrophic culture strategy for algal biomass and lipid production. *Bioresource Technology*, *103*(1), 484–488. https://doi.org/10.1016/j.biortech.2011.09.122

Zoni, V., Khaddaj, R., Campomanes, P., Thiam, R., Schneiter, R., & Vanni, S. (2020). Lipid Droplet Biogenesis is Driven by Liquid-Liquid Phase Separation. *SSRN Electronic Journal*, 1–30. https://doi.org/10.2139/ssrn.3526890